Molecular signature of domestication in the arboviral vector *Aedes aegypti*

Authors: A.N. Lozada-Chávez [1], I. Lozada-Chávez[2], N. Alfano[1]‡, U. Palatini[1]‡, D. Sogliani[1], S. Elfekih[3], T. Degefa[4], M.V. Sharakhova[5], A. Badolo[6], Patchara S.[7], M. Casas-Martinez [8], B.C: Carlos[9]‡, R. Carballar-Lejarazú[1]‡, L. Lambrechts[10], J.A. Souza-Neto[9,]‡, M. Bonizzoni[1]*

Affiliations:

[1] Department of Biology and Biotechnology, University of Pavia, Italy

[2] Institute of Computer Science and Faculty of Mathematics and Computer Science, University of Leipzig, Germany

[3] Australian Centre for Disease Preparedness-ACDP, CSIRO Australia

[4] School of Medical Laboratory Sciences, Institute of Health, Jimma University, Jimma, Ethiopia

[5] Department of Entomology and the Fralin Life Science Institute, Virginia Polytechnic and State University, Blacksburg, VA 24061 USA;

[6] Laboratoire d'Entomologie Fondamentale et Appliquée, Université Joseph Ki-Zerbo, Burkina Faso

[7] Department of Medical Entomology, Faculty of Tropical Medicine, Mahidol University, Thailand

[8] Centro Regional de Investigación en Salud Pública, Instituto Nacional de Salud Pública, Tapachula, Chiapas, México

[9] São Paulo State University (UNESP), School of Agricultural Sciences, Department of Bioprocesses and Biotechnology, Multiuser Central Laboratory, Botucatu, Brazil; São Paulo State University (UNESP), Institute of Biotechnology, Botucatu, Brazil

[10] Institut Pasteur, Université Paris Cité, CNRS UMR2000, Insect-Virus Interactions Unit, Paris, France

‡current address:
N.A.: Human Technopole, Viale Rita Levi-Montalcini 1, 20157, Milan, Italy
U.P: Laboratory of Neurogenetics and Behavior, The Rockefeller University, New York, NY, USA
RCL: Department of Microbiology & Molecular Genetics, University of California, Irvine, CA 92697-4025, USA
B.C.C.: São Paulo State University (UNESP), School of Agronomy, Crop Protection Department, Research group on Integrated pest management (AGRIMIP), Botucatu, Brazil;
J.A.S.N.: Department of Diagnostic Medicine/Pathobiology, College of Veterinary Medicine, Kansas State University, Manhattan, Kansas, USA

*Corresponding author, email: m.bonizzoni@unipv.it

Abstract

Background

Domestication is a complex, multi-stage and species-specific process that results in organisms living close to humans. In the arboviral vector *Aedes aegypti* adaptation to living in proximity with anthropogenic environments has been recognized as a major evolutionary shift, separating a generalist form, *Aedes aegypti formosus* (Aaf), from the domestic form *Aedes aegypti aegypti* (Aaa), which tends to deposit eggs artificial containers and bite humans for a blood meal. These behaviors enhance the mosquito vectorial capacity. The extent to which domestication has impacted the *Ae. aegypti* genome has not been thoroughly investigated yet.

Results

Taking advantage of two forms' distinct and historically documented geographic distributions, we analyzed the genomes of 634 worldwide *Ae. aegypti* mosquitoes. Using more than 300 million high-confidence SNPs, we found a unique origin for all out-of-Africa *Ae. aegypti* mosquitoes, with no evidence of admixture events in Africa, apart from Kenya. A group of genes were under positive selection only in out-of-Africa mosquitoes and 236 genes had nonsynonymous mutations, occurring at statistically different frequencies in Aaa and Aaf mosquitoes.

Conclusion

We identified a clear signal of genetic differentiation between Aaa and Aaf, circumscribed to a catalogue of candidate genes. These "*Aaa molecular signature*" genes extend beyond chemosensory genes to genes linked to neuronal and hormonal functions. This suggests that the behavioral shift to domestication may rely on the fine regulation of metabolic and neuronal functions, more than the role of a few significant genes. Our results also provide the foundation to investigate new targets for the control of *Ae. aegypti* populations.

Keywords

Aedes aegypti, genome, population differentiation, domestication, selection, local adaptation, vector-borne diseases

Background

The complex and multistage process that brings animals to live in proximity with anthropogenic environments has had a tremendous impact on both animals and human evolution since the Neolithic time when humans started to breed animals as food or commodity sources, protection, transportation, and company (1). For animals such as sheep, goats, cattle, chinchilla, American minks and shrimp domestication has been a human-driven process (2). For other species, domestication has been a self-selective natural process, which has resulted in an inherited attraction and adaptation to anthropogenic environments (2). A recognized consequence of domestication is exposure to zoonotic diseases because the domesticated animal may act as a reservoir or an amplifier of pathogens mainly acquired through interaction with wildlife (3).

The primary vector of arboviruses worldwide, the mosquito *Aedes aegypti*, exists as two different subspecies: the generalist *Aedes aegypti formosus* (Aaf) and the domesticated *Aedes aegypti aegypti* (Aaa). The distinction between the two subspecies has epidemiological relevance because Aaa tends to have a higher vectorial capacity than Aaf mosquitoes due to its behavior patterns of domestication, such as aptitude to oviposit in clean water of artificial containers and preference to blood feed on humans, and its higher vector competence for arboviruses (4–6). The two subspecies are distinguished at the phenotypic level, with Aaf a darker body color than Aaa (7,8). However, body color is not a binary phenotype, resulting in uncertainty (8,9).

Aedes aegypti is native of Africa and diverged from its closest relative, *Aedes mascarensis,* between 4 to 15 million years ago (MYA) (10). Nowadays, *Ae. aegypti* can be found throughout the tropical and subtropical regions of the world, but its geographic populations are not homogenous in terms of domesticated behaviors. Out-of-Africa populations, which originated through the

transatlantic slave trade from African populations, preferentially bite humans and lay eggs in freshwater of human-made containers (11). African populations tend to be generalist. While it is debatable when and which are the ecological drivers that caused this shift (6,12,13), genetic data based on microsatellite markers and exome sequencing have revealed a clear genetic differentiation between the two morphological subspecies, supporting a single sub-speciation event that probably occurred in West Africa, with the absence of gene flow between out-of-Africa domesticated and African generalist mosquitoes for at least 500 years (6,10,13–17). However, in a few African locations such as Kenya, Angola and urban sites of West Africa, *Ae. aegypti* mosquitoes that preferentially bite humans are sampled, suggesting recent reintroductions from out-of-Africa mosquitoes leading to admixture, persistence of descendants from the ancestral Aaa population of West Africa or incipient and independent domestication events (6,12,16,18).

It has long been speculated that domestication has strong genomic bases in *Ae. aegypti* because this species appears to have a high genetic diversity on a micro-geographic scale, and it is known to be fast evolving (16,19–21). However, the extent of the molecular differentiation in the genomes of the two subspecies in relation to biological functions associated with the behavioral switch to domestication have not been extensively investigated yet. Most efforts have been focused on identifying specific genes linked to hallmarks of domestication such as host-seeking behavior or insecticide resistance, the latter being a side effect of recurrent insecticidal interventions to control mosquito populations (22–24), based on the differential expression across *Ae. aegypti* populations (25–28) and/or the presence of nonsynonymous variants within a few target loci, including genes encoding for detoxification enzymes (*e.g.*, P450s) (23), neurotransmitter receptors (*e.g.*, Ir8) (29), the para sodium channel gene (*e.g.*, *kdr* mutations) (23,30,31), and odorant receptors (*e.g.*, AeOR4) (6).

Here, we present a comprehensive screening of genomic features in *Ae. aegypti* associated with adaptations to microgeographic and expected/recorded domesticated behaviors after its subspeciation event from the comparative analysis of the genomes of 123 out-of-Africa and 511

125 African mosquitoes. Among these genomes, we identified more than 300 million high-confidence
126 SNPs, which we used to assess population structure and test for signatures of molecular evolution.
127 Our analyses led to circumscribing the genetic basis of domestication to a catalogue of candidates,
128 which are strongly differentiated between Aaa and Aaf mosquitoes.
129

130 ## Results

131 ### 300 million high confidence SNPs detected across 634 worldwide *Ae. aegypti* genomes

132 We analyzed the complete genome of 694 *Aedes* spp. mosquitoes, including 4 *Ae.*
133 *mascarensis* and 21 *Ae. albopictus* samples. After removing datasets with low-quality mapping or
134 molecular identification as either *Ae. albopictus* or *Aedes simpsoni*, we obtained a final dataset of
135 634 *Ae. aegypti* genomes divided into two major geographical groups: African samples and out-of-
136 Africa samples (**Table 1, Fig. 1)**. Based on the presence or absence of the *Nix* gene, 192 and 395
137 mosquitoes were classified as males and females, respectively. Since the DNA of sperms can be
138 stored in female spermatheca, the remaining 47 individuals with partial coverage (2-44%) of the
139 *Nix* gene were considered females.

140 We identified a total of 322,552,899 high-confidence SNPs across the 634 *Ae. aegypti*
141 genomes by using two variant callers to recalibrate of our initial predicted SNPs dataset (~207
142 million) and ~485 thousand SNPs from ten published datasets (see Methods). We found no
143 statistical difference in the number of SNPs between males and females (t-test=2.75, $p>0.05$), while
144 SNPs number correlated with the length of chromosomes (length of chromosome 2: 2473 Mbs,
145 44.88% of total number of SNPs; length of chromosome 3: 409 Mbs, 37.71% of total number of
146 SNPs and length of chromosome 1: 310 Mbs, 26.40 % of total number of SNPs, rank coefficient
147 correlation > 0.87, $p<0.005$). SNP distribution does not fit a model of "random distribution" across
148 the chromosomes (chi-square test, $p>0.1$), but SNP density is highest at the telomere and decreases
149 towards the centromere in all three chromosomes. Due to the highly repetitive nature of the *Ae.*

aegypti genome (32), we distinguished between SNPs located in repetitive (R-SNPs) and non-repetitive (NR-SNPs) sequences. As expected, the number of biallelic and multiallelic R-SNPs (223 million) is higher in comparison to NR-SNPs (91 million), with no significant differences found in these trends for African and out-of-Africa populations (t-test=1.3, p>0.05). NR-SNPs are mostly located in intergenic regions (48%) and introns (43%), and to a lesser extent within exons (9%); whereas R-SNPs are equally distributed across introns and intergenic regions. Further analyses in this study are focused on the NR-SNPs dataset.

Among tested genomes, we identified 95 close relatives that represent >50% of individuals from six African populations, including Thiès (THI), Bundibugyo (BDB), Kichwamba (KIC), Virhembe (VIR), Bénoué (BEN), and Rabai (RAB), leaving a dataset of 539 *Ae. aegypti* genomes for which we performed a Principal Component Analysis (PCA). We recovered four well defined clusters representing three metapopulations from Africa (Western, Central-Eastern, and Eastern regions), and one from non-African populations, but we did not identify any cluster with mosquitoes that were previously described as "domesticated" in Rabai (6). A second PCA including all 634 mosquitoes showed RAB-related individuals are those with a closer affiliation to out-of-Africa mosquitoes (**Fig. 1B**). These results highlight that "domesticated" Rabai mosquitoes are inbred. Based on these results, we included all individuals from RAB, subdividing them into the "domesticated" (RABd) or "feral" (RABs) group, resulting in a final dataset of 554 *Ae. aegypti* genomes.

High genetic diversity and rare variants are more common in African populations

Among the 554 *Ae. aegypti* genomes, we detected 314,365,358 high-confidence SNPs; 81% are biallelic and 19% multiallelic. The average number of variants (R-SNPs, NR-SNPs) *per* population (46±16 million) represents 3.60% of the total variation detected in the genome, with a difference between African (3.99%) and out-of-Africa (2.02%) populations (**Table 1**). This can be

explained by the presence of almost two-fold more variants in African (51.91±13.72 million) than in out-of-Africa (25.84±1.90 million) populations (unpaired Wilcoxon signed rank test, p=0.000196), as previously observed (13, 18). Within African populations, the Western (SEN, BFA, GHA) and Eastern (KEN) regions have a similar number of variants (56.51±11.69 and 56.06±11.94 million, respectively), which is higher than that detected in Central populations (51.16±11.19 million). Conversely, out-of-Africa populations not only have less variants (25.84±1.90 million), but also less variance in the number of variants across them.

Mean nucleotide diversity (π) and Tajima's D (D) estimates were calculated with a non-overlapping sliding window of 10kb across chromosomes and populations to identify demographic changes. On average, π is found to be higher in African (0.67±0.33) than out-of-Africa (0.34±0.09) populations. Also, populations from Central and West Africa have more genome intervals with negative Tajima's D values on each chromosome, which are more concentrated towards the telomeres (63% of all sliding windows). Both estimates indicate that high genetic diversity and rare variants are more common across African populations, suggesting novel mutations due to population expansions. Conversely, NGY, RABd and out-of-Africa populations have more genome intervals with positive Tajima's D values, along with a reduced number of rare variants and nucleotide diversity (lower π values), suggesting a pervasive effect of bottlenecks or inbreeding due to one or repeated population contractions. These results and trends are robust to estimates with different sliding window sizes.

Unique origin for out-of-Africa mosquitoes and no evidence of incipient domestication or current admixture events between African and out-of-Africa populations beyond Kenya

Using a set of 1,530,512 biallelic SNPs that are shared across 80% of the 554 genomes, with no linkage disequilibrium and a minor allele frequency (MAF) of 0.01, we performed admixture analyses (K=3-13) (**Fig. 1C**) and compared pairwise fixation indexes (Fst) as a measurement of population genetic divergence and evaluating the presence of local introgression. Additionally, we

identified phylogenetic relationships among individuals and populations with two independent maximum likelihood (ML) trees that were reconstructed using exomic biallelic SNPs and *Ae. albopictus* as an outgroup (**Fig. 2**). Admixture analysis identified five well-defined clusters, representing one group from out-of-Africa populations and four African metapopulations from the Western (clusters 2), Western/Central (cluster 5), Central (cluster 3) and Eastern (cluster 4) regions (**Fig. 1C**). Furthermore, genetic separation is observed between populations west (Uganda, Western Kenya) and east (Eastern Kenya) of the Rift Valley. The human-feeding mosquitoes of the Senegalese NGY and THI populations (within cluster 2) and RABd (within cluster 9) formed distinct clusters. In the ML-phylogeny of individuals, RABd was found to form a single well-supported branch with JED mosquitoes (bootstrap=70%), as previously observed (10). This finding is supported by the lowest genetic divergence found between RABd and JED ($Fst_{\_RABd\text{-}JED}$=0.147±0.01) in comparison to the divergence found against other out-of-Africa ($Fst_{\_RABd\text{-}Aaa}$=0.179±0.091, range=0.156-0.214) and African populations ($Fst_{\_RABd\text{-}Aaf}$=0.183±0.013, range=0.148-0.231).

The ML-phylogeny for individuals (**Fig. 2A**) also identified a single well-defined branch including THI and NGY mosquitoes with all out-of-Africa populations (bootstrap <50%). The branch length of the nodes grouping THI and NGY is larger (7.27±0.66) than that grouping non-African mosquitoes altogether (4.45±1.24). Both THI and NGY show higher divergence with out-of-Africa populations ($Fst_{\_THI\text{-}Aaa}$: 0.127±0.12, range 0.113-0.175; $Fst_{\_NGY\text{-}Aaa}$: 0.104±0.12, range: 0.128-0.16), in comparison to the divergence found against other African populations ($Fst_{\_THI\text{-}Aaf}$: 0.048±0.025, range 0.004–0.02 and $Fst_{\_NGY\text{-}Aaf}$: 0.055±0.021, range 0-0.081). Additionally, Fst values estimated for THI and NGY with respect to mosquitoes from America, Asia and Oceania, which were colonized in a subsequent manner (11), showed a consistent high variance, whereas within genetic divergence in both THI and NHY populations was low (NGY: F_{IS}=0.015, THI: F_{IS}=0.013), with only one THI and two NGY mosquitoes grouping with Central Africa populations. Apart from NGY and THI, we observed grouping of mosquitoes within Africa in sampled

populations from West and East Africa, with extensive intermixing (*i.e.*, interleaving branches) in Central Africa, and no distinct separation among mosquitoes sampled in urban or rural/forestry sites, suggesting frequent gene flow in mosquitoes from these habitats. Results obtained from the ML-phylogeny for individuals were further confirmed by both the ML-populations phylogeny based on allele frequencies (33) and the F3 statistic, which tested genetic admixture among African populations and between African and out-of-Africa populations (34). THI, NGY and all out-of-Africa populations were found to form a single well-supported branch in the ML-populations phylogeny (bootstrap= 78%) (**Fig. 2C**). The phylogenetic relationship of both THI and NGY with out-of-Africa populations is not the product of admixture events, given that the F3 test was rejected in all cases (Z-cores values > -3.0). The same result was obtained when extending the F3 statistics to other African populations. On the contrary, there is evidence of admixture among African populations from geographically close regions, independently of their urban or forest location. The ML-populations phylogeny also showed that the amount of genetic drift is higher across out-of-African populations, in agreement with our findings of low genetic diversity and positive values of Tajima's D.

Signatures of local genetic adaptation is detected in out-of-Africa mosquitoes

Admixture and phylogenetic analyses confirmed the genetic separation between African mosquitoes and domesticated out-of-Africa samples and highlighted RABd, NGY and THI as the African samples most closely related to Aaa mosquitoes. To further identify patterns of molecular differentiation among our samples, we screened for outlier SNPs using the program *PCAdapt* (35). Among the 10,030 outliers detected, the majority were located within intronic (45%) and intergenic (26%) regions, while 27% mapped to protein-coding exons of 2,266 genes. In agreement with results from our phylogenetic analyses, apart from THI, NGY and RABd, all African populations grouped together and were separated from out-of-Africa mosquitoes (**Fig. 3**). The first three principal components (PCs) accounted for 95% of the data (one sample t-test for PCs, $p<0.001$;

pairwise t-test for populations, $p<0.001$). PC1 captured 6,041 outliers distributed across 1639 genes that support local adaptations for THI, NGY, RABd, RABs and out-of-Africa populations; PC2 and PC3 included 3,559 outliers in 986 genes highlighting local adaptations in NGY and eight Kenyan populations. The remaining PCs explain 5% of the data and identified 429 outliers across 233 genes indicating local adaptations in out-of-Africa populations.

The hallmark of domestication in *Ae. aegypti* is higher attraction to humans than animals, a phenotype that was used to classify Aaa and Aaf mosquitoes, prior to the discovery of Aaf mosquitoes preferentially blood-feeding on humans in Cape Verde and Senegal, and is regulated by chemosensory receptors (6,26,36). Among the 198 *Ae. aegypti* chemosensory genes, 32 had outliers. Relative to other functional categories, most genes with outliers were associated with functions such as protease activity (35 genes out of 292 genes), detoxification (29 genes out of 198 genes), immunity (62 out of 391 genes) or biosynthetic and metabolic processes, signaling and receptor activities, metal ion homeostasis and (GTPase) binding activities. All genes harboring outliers showed high genetic differentiation (sites average Fst≥0.09) and deviation from neutrality (Tajima's D: one sample t-test, m=0, $p<0.001$), suggesting signals of selection. Additionally, outliers in 306 genes resulted in nonsynonymous mutations, which occurred at a significantly different allele frequency in African and out-of-African mosquitoes in 236 genes, including the odorant receptor (OR) genes *OR91* and *OR86*, the ionotropic receptors (Ir) *Ir41g*, *7g* and *8a*; the gustatory receptor (GR) *9*; immunity genes as *Toll5A,* the gram-negative binding protein (GNBP) A2, the clip-domain serine proteases *CLIPE12*, and *CLIPE8*, and several genes with unknown functions (*i.e.* AAEL025393, AAEL001559, AAEL020878, AAEL022804, AAEL022666, AAEL019451, AAEL012825, AAEL012783, AAEL012268, AAEL010998, AAEL008698) (**Fig. 4**).

Genes associated with diverse neuronal functions are positively selected in out-of-Africa mosquitoes.

We further estimated selective constraints by calculating the ratio of non-synonymous (Ka) to synonymous (Ks) substitutions (dN/dS ratio) for the 13,503 *Ae. aegypti* genes that mapped SNPs in their protein-coding exons. We found 12,991 genes evolving under negative selection, which are mostly shared across all tested populations, with none of the five clusters identified offering an unambiguous distinction between Aaf and Aaa mosquitoes. By contrast, we found that most local adaptation across Aaa populations seems to be driven by 1,033 genes (from 9 clusters) out of the 5,242 genes that were found evolving under positive selection. We consider this set of 1,033 genes as "*Aaa molecular signature*" because they clearly differentiate African from out-of-Africa populations (**Fig. 5**). The "*Aaa molecular signature*" genes were distributed across the three chromosomes, encompassing the regions from 128.3 to 287.7 Mb and 284.5 and 344.8 Mb on chromosome 2, which harbor Quantitative Trait Loci (QTLs) previously linked to higher vector competence for Zika virus in mosquitoes from Guadeloupe vs Gabon (5). Chemosensory and immunity genes were the most represented ones among the "*Aaa molecular signature*" genes (**Fig. 5**). We detected several olfactory-associated genes evolving under positive selection across several out-of-Africa populations, including *Gr1* in JED and BNK; *Gr34* in JED and SAS; *Gr20* in SAM, TAP, SAS, and BNK; *Obp*jj7a in JED, SAS, and BNK; *Obp14* in JED; *Or13* in JED and SAS; *Or44* in TAP and SAS; *Or45* in JED, SAS and BNK; and *Or4* in TAP and JED. Across tested mosquitoes from Asia and/or America, signals of positive selection were found to be mostly local, with concordant results from the PCA-outlier analysis in *Gr1, Gr8, Gr20a, Ir7g, CLIB1* and *GPXH2*; the cytochrome P450 CYP6Z7, which has been frequently associated with resistance to pyrethroids (37–39), showed pervasive positive selection, showed pervasive positive selection in remarkable contrast to most negatively selected P450 genes, further underscoring its physiological role and the significance of these results.

Among the "*Aaa molecular signature*" genes is notable the presence of genes associated with neuronal and hormonal functions such as the N-methyl-D-aspartate (NMDA) receptor (AAEL008587), which belongs to the family of ionotropic glutamate receptors playing a major

signaling role in the central nervous system and in neuromuscular junctions (40); the *capa* gene (AAEL005444) belongs to the PK/PBAN family of neuropeptides, which in *Drosophila melanogaster* encodes for pyrokinin-1 and periviscerokinins (41), and has been shown to regulate diverse physiological functions ranging from feeding behavior (42) to the regulation of water balance (43); tomosyn (AAEL006948), a motoneuron receptor that influences homeostatic synaptic plasticity (44); the synaptic vesicle protein synaptotagmin (AAEL001167) (45), and several G-protein coupled receptors (GPRs), a category of proteins enriched among *Anopheles gambiae* brain peptides (46).

Endogenous Viral Elements contribute to differentiate out-of-Africa and African mosquitoes

Recent experimental evidence expands the immunity toolkit of *Ae. aegypti* to nonretroviral endogenous viral elements (nrEVEs), which interplay with the piwi-interacting (pi) RNA pathway to control cognate viral infections (47,48). The genome of *Ae. aegypti* harbors 252 nrEVEs (hereafter *reference* nrEVEs), > 50% of which are at least 4 MYA being shared with *Ae. mascarensis* (47,49). *Reference* nrEVEs coexist with 64 "*new*" nrEVEs, which are exclusively detected in wild mosquitoes, and their distribution significantly differed in African and out-of-Africa mosquitoes. A total of 5 *new* nrEVEs (Guato_2, CFAV_EVE-4, CFAV_EVE_1, CFAV-EVE-5, *Aedes aegypti* toti_like-7) are unique of out-of-Africa mosquitoes and, overall, *new* nrEVEs have a higher nucleotide identity to cognate viruses than *reference* nrEVEs. With the exception of three integrations from the *Liao Ning* virus belonging to the *Seadornavirus* genus (Reoviridae family), which includes emerging pathogens (50), all *new* nrEVEs are from limited number of ISVs. We also observed frequent rearrangement events following integration, especially for nrEVEs with similarity to flaviviruses that map in piRNA clusters, supporting the conclusion that nrEVEs contribute to the genetic flexibility of *Ae. aegypti* piRNA clusters.

DISCUSSION

Domestication is a complex, multifactorial and species-specific process traditionally associated with vertebrates, among animals. Still, domestication events have also occurred in a few invertebrates such as shrimps (*Panaeus* spp.), the silk moth *Bombyx mori* and *Ae. aegypti* (1,51,52). In the case of *Ae. aegypti*, it took only a few hundred years for the species to become globally invasive and human specialist (11,12). *Aedes aegypti* domestication process has resulted in changes on different aspects of its bionomics (e.g. vector competence, reproductive behavior and host feeding preferences) and, by consequence of human interventions, in insecticide tolerance in just a few thousand years (6,12,24).

This work represents the most comprehensive effort to date to identify genomic variants and footprints of genomic selection tracing the evolutionary divergence and behavioral switch of *Ae. aegypti* populations to domestication. To revisit this matter with unprecedented phylogenetic resolution, we used the high-quality reference assembly AagL5 (32) and the genomes of 511 African and 123 out-of-Africa mosquitoes that were sampled and sequenced from 14 countries across four continents. From >300 million high-confidence SNPs detected throughout the whole *Ae. aegypti* genome, we found protein-coding variants that can significantly differentiate Aaa from Aaf mosquitoes. We call this group of genes "*Aaa molecular signature*" genes. A total of 236 "*Aaa molecular signature*" genes harbor nonsynonymous mutations that occur at statistically different frequencies between Aaa and Aaf mosquitoes. Thus, they could be used to distinguish the two *Ae. aegypti* subspecies molecularly. In the following, we discuss the population structure context under which these "*Aaa molecular signature*" genes were identified, highlighting their association with expected (olfaction) and novel functional hallmarks of domesticated behaviors in *Ae. aegypti*.

Our genetic structure and phylogenetic analyses performed over 1.5 million biallelic and non-redundant SNPs, led us to confirm a major genetic divergence between African and out-of-Africa populations, with the former being clearly genetically structured into Western, Western/Central, Central and Eastern metapopulations. These results are strongly supported by the

pairwise-Fst genetic distances obtained across all populations, with the unique exception of RABd. We consistently found that RABd formed a cluster, which separated from other African populations and was phylogenetically more closely related to, and shared the lowest genetic divergence with, JED, in comparison to all other tested populations. Empirical observations of closer relatedness between Aaa populations and behaviorally divergent ‘‘domestic’’ and ‘‘forest’’ mosquitoes of Rabai have been reported previously, with contradicting hypotheses concerning the origin of such ‘domesticated behavior’ (6,10,16,53,54). The findings of our study provide compelling evidence for a “back to Africa” event, indicating a recent reintroduction from Saudi Arabia into Kenya of Aaa mosquitoes, which remained localized as indicated by extensive inbreeding.

Our admixture and PCA analyses also provide strong support for the separated genomic clustering of the human-feeding mosquitoes sampled from the Senegalese NGY and THI populations (6). Results from ML-phylogenies further showed that NGY and THI are closely related to out-of-Africa mosquitoes. Importantly, not only the branch grouping both THI and NGY with out-of-Africa populations is basal to all African population, but it also supports a high genetic divergence between NGY/THI and out-of-Africa populations when compared to other African populations, which is consistently confirmed by all pairwise-Fst distances. We also demonstrate that the close phylogenetic relationship of both THI and NGY with Aaa populations is not the product of admixture events, given that the F3 test was rejected in all cases. F3 results discarding admixture with out-of-Africa populations extend to all tested African mosquitoes. Altogether, these findings are consistent with inferring that NGY and THI derive from an ancestral domesticated population, rather than representing recent re-introductions and/or admixture events between African and out-of-Africa mosquitoes (9,11,13–15,18,55).

The genome-wide SNP divergence between African and out-of-Africa populations, which agrees with previous studies (6,13,16,18), is further endorsed by the differential clustering of nrEVEs between the two subspecies, with 5 nrEVEs being exclusive of out-of-Africa populations. These Aaa-specific nrEVEs belong to a group of 64 novel, and PCR-validated, nrEVEs that we strongly

suggest being the outcome of recent integration events given their higher nucleotide identity to cognate viruses. The population structure that we found, meaning a unique origin for all out-of-Africa domesticated mosquitoes with NGY and THI representing ancestral domesticated mosquitoes and no current admixture between African and out-of-Africa mosquitoes or new introductions of Aaa into Africa, except for RABd, was the basis to continue in the identification of genomic variants and footprints of genomic selection between out-of-Africa domesticated and generalist African mosquitoes. To test whether or not switches to long enduring domesticated behaviors in *Aedes aegypti* have a strong and multi-loci genomic basis, we joined two well-known approaches: first, we identified genomic variants more strongly associated in all populations of the two subspecies than expected only by genetic drift; second, we identified all those positively selected protein-coding variants that can unambiguously differentiate patterns of adaptation in African versus out-of-African populations. We found that the genetic divergence between Aaa and Aaf is highest in a group of genes from the prediction of both approaches, that we call "*Aaa molecular signature*" genes. Given that results from these estimations are sensitive to the number of populations that are tested and their grouping, we performed our analyses on all populations and statistically validated population divergence prior to calling outlier SNPs. While some "*Aaa molecular signature*" genes may reflect local adaptation independently of domestication, in gene families associated with functional redundancy, local adaptation signals may still be domestication signals.

Our candidate "*Aaa molecular signature*" genes include olfactory genes, which mediates sensing of volatiles, a function used by *Ae. aegypti* females to locate both a host for blood feeding and a breeding site for oviposition (58,59). Olfaction is governed by multi-gene families and has a highly redundant organization in *Ae. aegypti*, with multiple receptors in the same neuron and individual variability, which is different from the canonical organization "one receptor-one neuron-one glomerulus" observed in *Drosophila melanogaster* (58). This level of redundancy increases the breath and the flexibility of volatile perception, and it may be linked to local adaptation at the

genomic level. Despite this redundant organization, a few candidate receptors have been identified as having a major role because of their either ubiquitous co-receptor function (i.e., *Orco*, *Ir8a*, *Ir25a,* and *Ir76b*) or prevalent sensing of human-relevant compounds, such as sulcatone by *Or4*, CO_2 by *Gr3*, and lactic acid by *Ir8a* (26,60-63). We identified pervasive negative selection in *Orco* and *Gr3*, underscoring their physiological role. Consistent with the hypothesis that functional redundancy may entail local adaptation, we detected strong genomic signals of local adaptation across several olfactory-associated genes such as *Gr1* in RABd and all out of Africa; *Gr20* in Kenyan populations (MBK, ARA, GND, KYB, KWA, SHH, and RABd, RABs) and NGY; O*r26* in THI, NGY, RABd, RABs; *Or44* in TAP and SAS; *Or45* in JED, SAS and BNK; *Or86* in RABd and out of Africa; *Or4* in TAP and JED; *Gr8* and *Gr20a* in Kenyan populations (MBK, ARA, GND, KYB, KWA, SHH, and RABd, RABs) and NGY; *Ir7g* in THI, NGY, both RAB, and out of Africa populations. *Or4* is particularly significant as different *Or4* alleles are known to circulate across *Ae. aegypti* populations, with levels of *Or4* expression being strongly predictive of preferential attraction to humans (26). Here, we circumscribed our analyses to coding sequences, thus we are possibly missing variants that could regulate *Or4* expression. Such analyses would require complementary transcriptomic data assessing gene expression and extensive functional validation, which are beyond the scope of our current work. In the co-receptor *Ir8a*, which is expressed specifically in antennal neurons and is required for perception of lactic acid, a component of human sweat (60), we identified nonsynonymous mutations occurring at significantly different frequency in Aaa and Aaf mosquitoes. In NGY and THI, which are African mosquitoes that behave like Aaa in their preference for humans (6), these mutations appear at frequencies which are intermediate between those detected in Aaa and Aaf mosquitoes, underscoring their significance and pointing to functionally assessable targets for future endeavor.

As expected, our list of "*Aaa molecular signature*" genes include additional genes belonging to major gene families such as detoxification, immunity, and proteases, which have been shown to impact host seeking behavior, vector competence and overall response to external stimuli

435 (6,32,64,65). Notable examples include *Toll5A,* which interacts specifically with Spaetzle1C resulting
436 in regulation of immunity and, primarily, fatty acid metabolism (66,67), as well as several clip-
437 domain serine proteases, which are upregulated following *Ae. aegypti* infection with different
438 pathogens (68,69). Although >50% of "*Aaa molecular signature*" genes lack a functional annotation,
439 also notable is the presence of genes associated with broad hormonal and neuronal functions such
440 as the NMDA receptor, the *capa* gene, tomosyn and synaptotagmin (41–43,45), suggesting that the
441 behavioral shift to domestication may rely on the fine regulation of metabolic and neuronal
442 functions, more than the role of a few major genes. In support to this hypothesis, domestication in
443 rabbits, which occurred rapidly in the past 1500 years, resulted in a shift in primarily SNPs nearby
444 genes associated with brain and neuronal development (1,70). Additionally, a mutation affecting the
445 *thyroid-stimulating hormone receptor*, which controls photoperiodic diapause and reproduction, is
446 widespread but not fixed in domestic chickens (71,72), and candidate domestication genes in the
447 silkworm (*Bombyx*) include genes involved in energy metabolism, reproduction and silk gland
448 activity (69).

449 Altogether, our findings robustly suggest that domesticated behaviors in *Ae. aegypti* have
450 evolved by shifts in allele frequencies and codon selection at many loci, owing to diverse selective
451 pressures caused by local adaptations to microgeographic and anthropogenic changes worldwide.
452 In particular, selection on olfactory genes and their related nonsynonymous variants, which are
453 expected to be relevant for generating the behavioral switch in *Ae. aegypti* to domestication, are
454 found to be strongly influenced by genetic background and population history. The genetic diversity
455 richness of the generalist African populations found in both repetitive and non-repetitive regions
456 throughout the whole genome strongly suggests that retention of ancestral polymorphisms is likely
457 the main genetic source for the evolution of complex evolutionary dynamics in the domesticated
458 behaviors of *Ae. aegypti*. The absence of introgression between the Aaa and Aaf populations
459 analyzed here, and the 2-fold reduction of SNPs, nucleotide diversity, rare variants, and high genetic
460 drift that we found across out-of-Africa populations strongly endorse this hypothesis, although

other genomic events, recent retention of polymorphisms due to local introgressions and convergent evolution on certain loci are not to be discarded (*e.g.*, (73)). Retention of ancestral allelic variants based on microsatellite markers was suspected to occur in *Ae. aegypti* (13,18,20), but was only reported in other human-feeding mosquitoes recently, such as *Anopheles gambiae* (74–77), *Culex nigripalpus* (78), and *Cx. quinquefasciatus* (79). Particularly notable is the presence of alternative allelic variants at low frequency (*i.e.*, "standing variation") in the same protein-coding genes that we found to be evolving under nearly neutral or weak (positive/negative) selection across most African populations (**Fig. 5c**), which may be maintained for longer periods of time beyond neutral expectations (80). This is the first large-scale observation of selection over preexisting standing variation in *Ae. aegypti*, a phenomenon that has been also reported in *Daphnia* (79) and a few other organisms (82–85). By selecting from a rich stock of ancestral and weakly evolving standing variants from African populations, we observe that some of the *"Aaa molecular signature"* genes such as the odorant receptor gene AAEL000616 found within modules linked to active periods or sleep-like states (86), the chymotrypsin JHA15 (AAEL001703) found to be highly expressed before a blood meal (87), and the immune-related recognition gene AAEL019958 found to be exclusively expressed in ovaries of female mosquitoes (88), and several chemosensory genes have switched to directional selection in several out-of-Africa populations, where the fast emergence of novel adaptations can be easily promoted by the redundant organization of olfaction to cope with novel geographical and anthropogenic evolutionary pressures.

Relative to recent efforts in other human feeding mosquitoes, our work provides a unique resource for the study of population genetic structure and genome selection on a microgeographic scale for one of the fastest evolving arbovirus vectors worldwide. We also pinpoint to further candidate genes involved in neuronal functions as targets of genetic manipulation and neurogenetic approaches recently developed for mosquitoes (58,89–92).

Methods

Mosquito samples

We studied the whole genome sequence of 694 *Aedes* spp. mosquitoes. This sample size included previously published WGS data of *Ae. aegypti*, *Ae. mascarensis* and *Aedes albopictus* (6,10,47,93) and WGS data of 97 *Aedes* spp. mosquitoes that we processed from Burkina Faso, Ethiopia, Brazil, Saudi Arabia, Russia, Cameroon and New Caledonia. With the exception of New Caledonia from where we received eggs through the 'Infravec2' project (https://infravec2.eu/), from all other sites we received adult mosquitoes preserved in ethanol 70%; these mosquitoes had been sampled either as larvae from tires, backhoe buckets and various surrounding larval habitats or as adults through 'BG-sentinel' traps. Mosquitoes from Cameroon are from a colony established from eggs collected in Bénoué; females were sampled at the 12th generation after colony establishment. Genomic DNA was extracted from individual mosquitoes using the Wizard Genomic DNA Purification Kit, according to the manufacturer's protocol, at the University of Pavia for all specimens, apart from mosquitoes from Brazil, which were processed *in loco.* Genomic DNA was sent to Macrogen for individual DNA library preparation with TruSeq DNA PCR-free reagents and sequencing to a minimum of 20X coverage (24X on average) in paired-end 150 bp reads with the Illumina HiSeq X Ten platform. FASTQ files of all WGS datasets were subjected to quality control by using FASTQC v0.11.9 (94). Sequencing data were deposited to the NCBI SRA under the accession BioProject ID: PRJNA943178.

Alignment to the reference genomes

Raw reads of each of the 694 WGS datasets were trimmed using Trimmomatic v0.39 (95), then the 21 *Ae. albopictus* WGS data were aligned to the *Ae. albopictus* Foshan FPA genome assembly (96), the remaining WGS data were aligned to the current *Ae. aegypti* reference genome assembly, AaegL5 (32); both assemblies were downloaded from VectorBase (https://vectorbase.org/). The BWA MEM algorithm v0.7.17.r1188 was used for all alignments (97). For each sample, genome mapping statistics were calculated with Qualimap v2.0 (98) and alignment quality statistics were

obtained with bamtools (99). For WGS data mapped to the *Ae. aegypti* genome, gene coverage was calculated for the 14,677 genes reported in AaegL5 with the program mosdepth v0.2.9 (100). For a total of 35 samples, less than 50% of the reads aligned to AagL5. To clarify this result, we reconstructed the sequences of the ribosomal Internal Transcribed Spacer 1 and 2 (ITS1 and ITS2) of these 35 sampled by using the *LT_finder* script of the ViR pipeline (49) and the 5.8S rRNA sequence of *Ae. aegypti* (accession M95126, region coordinates 574-755 in AagL5) as reference. The reconstructed ITS1-ITS2 sequences were then blasted, with *blastn*, against the 'nt database' of NCBI with default parameters through the BLAST webserver (https://blast.ncbi.nlm.nih.gov/) to confirm species identity. All samples from Russia and Ethiopia showed the highest identity to ITS sequences of *Ae. albopictus* (identity>97.24%, 100% query coverage, and E-value of 0) or *Ae. simpsoni* (identity>97.66%, 100% query coverage, and E-value of 0), respectively. WGS data from 9 additional mosquitoes had low (≤2 reads) and/or partial coverage (≤45%) to AaegL5, but their ITS1-ITS2 reconstructed sequence did not yield results when searched against the 'nt database' of NCBI, suggesting either uncharacterized species or sequencing quality issues. To avoid biases in the analysis, these WGS datasets were excluded resulting in final dataset of 634 mosquito genomes from 39 populations, for which ≥96% of reads mapped to AagL5. In these WGS samples, 95% of the 14,677 *Ae. aegypti* genes were covered with ≥5 reads; the remaining 5% of genes, which were covered with ≤4 reads, mapped in *contigs* that have not been assigned to any chromosome yet.

Females were identified among these 634 mosquitoes by the complete absence of coverage on *Nix* (AAEL022912); males are expected to have coverage over the protein coding region of *Nix* (≥1 read) (101), which was estimated with Samtools v1.4 (102). In presence of coverage over *Nix,* we also verified coverage of the *myo-sex* gene (AAEL021838) to further support the sex association to males. To verify amplification of the *Nix* gene from sperms stored in female spermathecae, we sampled males, virgin females and females collected after copulation. DNA of each of these samples was extracted with the Wizard Genomic DNA Purification Kit (Promega) following

manufacturer recommendation. DNA was amplified with a nested PCR using in the first PCR primers Nix_aeg_PCR-F: 5'-ACGGAAGAGCGAATTGCACA and Nix_aeg_PCR-R: 5'-GTCAAACCGTCTGAGCGTCT and in the second reaction primers Nix_aeg_nPCR-F: 5'-AGCGTGCTTCAGAATAATTACGG and Nix_aeg_nPCR-R: 5'-GTTTTGATGCGGTGAGTGCC. PCR reactions were assembled using the DreamTaq Green PCR Master Mix (Thermo Scientific) following manufacturer's instructions. 1 uL of DNA extract was added to reach a final volume of 25 uL. PCR reactions were performed in a thermal cycler (Eppendorf™ Mastercycler Nexus Gradient) with, after an initial denaturation for 3 minutes, 35 cycles at 95°C for 30 s, 52.4°C or 53.3°C for 30 s for the first or second PCR, respectively, and an extension of 25 s at 72°C, followed by a final extension for 10 minutes at 72°C. PCR products were visualized using a Bio-Rad Gel Doc TM EZ Imager following electrophoresis in a 2% (w/v) agarose gel.

Recalibration of alignments and variant discovery

The 634 WGS data mapped to the *Ae. aegypti* genome (AagL5 assembly) were further processed following the best practices recommendations from the Genome Analysis Toolkit (GATK) (103,104). First, the program Picard v2.23.0 (Broad Institute, 2019; https://broadinstitute.github.io/picard/) was used to sort aligned reads and mask optical duplicates. Then, local realignments were performed with the GATK package v3.81.08 (105) over regions mainly characterized by indels (insertions and deletions) and read mate coordinates of realigned reads were recalculated with the Picard program. Finally, the Base Quality Score Recalibration (BQSR) was calculated for each alignment with the GATK package. To improve alignment during the recalibration step, we provided to GATK a set of known indels and Single Nucleotide Polymorphisms (SNPs). This set of variants was built with two different approaches: 1) known SNPs from literature and 2) *de novo* SNPs estimates for our sequenced mosquitoes through bioinformatic analyses. Both procedures are described next.

SNPs collected from literature

An initial collection of 485,431 SNPs was obtained in a variant calling format (vcf) file from nine published studies (23,106–113). From this collection, 112,969 SNPs (23.27%) have experimental support such as high-throughput genotyping chip 'Axiom_aegypti1' (106–110), while the remaining 372,462 SNPs (76.73%) were estimated only through bioinformatic analyses (23,111–113). The genomic coordinates of all nine SNPs datasets were re-mapped from the *Ae. aegypti* assembly AaegL3 to the AaegL5 version through the lift over strategy by the VectorBase website. A SNP dataset originated from exome analysis (13) was also added to our study. For this dataset, we performed a local lift over with the *Flo* pipeline to re-map all genomic coordinates from the AaegL1 to the AaegL5 assembly (114). We used the UCSC chain files (113), the gnometools package (114), and the pblat-cluster v36x2 (117,118) to accelerate the sequence search mapping across genome assembly versions. Finally, we used Crossmap (119) to perform the genomic conversion of coordinates for the set of known SNPs over AaegL5. Overall, after merging sites and removing overlapped redundant variants, from these 10 SNP datasets a total of 304,428 SNPs were mapped across 10,185 *Ae. aegypti* genes and 278 contigs annotated in AaegL5.

De novo SNP discovery

Two variant callers, GATK v3.8.1.0 (105) and Freebayes v1.3.1 (https://github.com/freebayes/freebayes) were applied to identify SNPs from each of the 634 WGS samples mapped to AagL5 to improve SNP prediction because both variant calling tools have a high false discovery rate (FDR) when compared to a true set of known SNPs (120–122) and both tools are known for scoring best at one, rather than in all, quality parameter measurements (120,123). We further implemented a strict filtering protocol for each set of identified variants to complement the power prediction of both variant calling tools and increase specificity and sensitivity. First, variant caller predictions were performed with GATK and Freebayes for each sample, separately.

Then, raw SNPs and indels calculated from Freebayes were extracted and filtered with: 1) a minimum deep coverage of 5 reads (DP≥5); 2) a minimum mapping quality of 20 (MQ≥20); 3) a minimum base quality of 20 (QUAL≥20) and 4) a minimum allele frequency ≥ 1% (maf≥0.01), as calculated with BCFtools (102). Filtering of the GATK called variants was implemented with the GATK protocol for SNPS: QUAL < 30.0, QD (QualByDepth) < 2.0, FS (FisherStrand) > 60.0, MQ (RMSMappingQuality) < 40.0, SOR (StrandOddsRatio) > 3.0, MQRankSum (MappingQualityRankSumTest) < -12.5, ReadPosRankSum < -8.0; for INDELs: QUAL < 30.0, QD < 2.0, FS > 200.0, ReadPosRankSum < -20.0). All SNPs with a close proximity of 10 base pairs to an indel and with a strong strand bias (p<0.001) were removed with BCFtools. Finally, we merged all sites and removed all overlapped redundant variants from the known and *de novo* approaches, which generated a final high-quality collection of 82,686,298 indels and 207,724,254 SNPs that we used in the recalibration step, as described above.

A refined variant caller prediction was performed only with the GATK protocol for all recalibrated alignments in each of the 39 populations, separately. Raw SNPs and indels were extracted and filtered with the same filtering parameters using GATK, as described previously. After this last filtering process, a total of 314,365,358 SNPs were obtained as the core dataset of our analyses, while indels were not considered in further analyses.

Pairwise relatedness of individuals in *Ae. aegypti* populations

We evaluated the *degree of relatedness* among the 634 individuals within each of the 39 populations and removed closely related individuals (*i.e.*, full siblings) to avoid any bias. To this end, we first removed all SNPs detected over repetitive regions of the *Ae. aegypti* genome by using the genomic coordinates reported by (32); and then we extracted all biallelic SNPs present in at least 90% of individuals within each population. Next, highly linked loci were eliminated using the function *snpgdsLDpruning* (ld.threshold=0.01) of the SNPRelated R package (124), and the corresponding

matrix of 'relatedness coefficients' (k) was generated with the Identity-by-Descent (IBD) measurement based on maximum likelihood estimation (MLE) by using the function *snpgdsIBDMLE* included in the same R package. Highly genetically related individuals were classified and filtered in each population using two conservative cutoffs for African and out-of-Africa populations, as previously suggested by (6): *first cousin and closer relationships* ($k \leq 0.05$) for African populations and *siblings* ($k \leq 0.20$) for out-of-Africa populations. We repeated this analysis by using a dataset of 1,000,000 randomly sampled SNPs across the whole genome per population, and manually compared both approaches by identifying the individuals, as well as the total number of individuals to be removed. Through this process, we removed 95 individuals, leaving a dataset of 539 individuals. Among these 95 related individuals, 15 corresponded to the previously called 'domesticated' mosquitoes of the Rabai population (6). To confirm the *relatedness groups* estimated with our protocol, an analysis on the covariance of genotypes was performed with the *pca* function of the plink v2.0 package. Based on this analysis, all domestic individuals from Rabai were reintroduced to our dataset, resulting in final set of 554 *Ae. aegypti* genomes for further analyses.

Distribution of SNPs and genetic diversity along the *Ae. aegypti* genome

Unless otherwise stated for all further analyses, we used *Ae. aegypti* genomic coordinates as reported in AaegL5 (32). We mapped the entire set of 314,365,358 filtered biallelic and multiallelic *Ae. aegypti* SNPs to compare the distribution of SNPs across each centromeric region and chromosome arms (*1q*, *1p*, *2q*, *2p*, *3q*, *3p*) and used a paired t-test to find significant difference between and among chromosome arms in African and out-of-Africa populations. We further estimated the total number of SNPs counts in chromosomes (hereafter 'chromosomal SNPs') or contigs (hereafter 'unassigned SNPs'), and, in each of these regions, we counted SNPs in exons, protein coding regions (CoDing Sequences, CDS) and untranslated (5'- UTR and 3'-UTR) regions and further split SNPs based on whether they occurred in repetitive (R-SNPs) or non-repetitive

regions (NR-SNPs) by using the function SelectVariants, options *intervals/excludeIntervals,* in GATK. R-SNPs counts are listed for Transposable Elements (TE), low complexity sequences and unclassified repeats.

Focusing on NR-SNPs, we measured genetic variance in terms of SNP density, genetic diversity (π) and Tajima's D using the VCFtools package (125). A genome-wide scan with different non-overlapping sliding windows (10kb, 50 kb, 100 kb, 250 kb, and 500 kb) was performed to calculate both basic statistical descriptors for genetic variation. Finally, we identified the presence of 'SNP singletons' (*i.e.*, a SNP present in one single individual of a population) with the VCFtools package (options *singletons* and *positions*) and estimated their counts and distribution across populations using a custom R script.

Population Genetics Analyses

Chromosomal biallelic SNPs that were found in at least 80% of all individuals were extracted and further filtered out using plink v2.0, to avoid sampling genotyping errors (126), if highly linked (option indep-pairwise: window size=50, step size=10, and R^2=0.1), having a MAF<0.01 or showing a significant deviation from Hardy-Weinberg equilibrium (HWE) (p<0.001). This procedure led to a total of 1,530,512 SNPs that were used to assess the genetic relationships across populations using the *pca* function of the plink v2.0 package, for admixture analysis using the ADMIXTURE software v1.3.0 (127), and to estimate F_{ST} population scores using VCFtools (125). As described in (128), we ran ADMIXTURE on all individuals and varied the number of genetic clusters (K) from 1 to 39 to identity the number of clusters that minimizes the cross-validation error. We performed the PCA and admixture analyses on different genomic scales (*i.e.*, WG, R, NR and exon regions) to test for differences in the distribution of genetic variation across the mosquito genome that might potentially induce distinct effects on the populations structure. For exon regions, 1,000 bootstrap replicates for every dataset with a cluster (*k*) value from 2 to 39 were carried out to

further support the identification of the optimal cluster number. A matrix of all-vs-all pairwise comparisons of the F_{ST} population scores was built using VCFtools and a custom PERL script to estimate the genetic divergence across populations. All populations were then grouped according to a *complete* hierarchical clustering by using an *euclidean* distance and 1,000 bootstrap replicates with the pvclust R package (129).

We further investigated the phylogenetic relationships among the 554 *Ae. aegypti* genomes by building a ML phylogenetic tree with all SNPs from exons of protein-coding genes that were present in 100% of individuals across all populations (named here as "core-exome SNPs); we define this phylogeny as "tree of individuals". This set of SNPs was transformed into a phylip format with the vcf2phylip program (https://github.com/edgardomortiz/vcf2phylip/blob/master/vcf2phylip.py) and the corresponding phylogeny was reconstructed with a GTR+CAT substitution model (-m ASC_GTRCAT) that includes an ascertainment bias correction for SNPs (ass-corr=lewis); the statistical robustness of the phylogeny was assessed with 1,000 bootstrap replicates using RaxML v8.2.12 . Using the same set of SNPs, we also derived a ML phylogenetic tree based on SNP frequencies estimated within each population; we define this phylogeny as "population tree". This tree was built with the TreeMix program after 1,000 bootstrap resampling of the dataset (33). For both phylogenetic trees, *Ae. albopictus* was used as an outgroup. The F3 statistics implemented in the TreeMix program (program *threepop*), which measures the covariance of the differences in allele frequencies among three populations, was used to test the genetic admixture of THI and NGY populations with respect to out-of-Africa populations. The association test of these populations is depicted in a tree topology of the type (A,B;C), where *C* is either THI or NGY, and *A* and *B* represent all possible combinations of the out-of-Africa populations. Genetic admixture was established based on z-scores as a test statistic and a conservative threshold (z-score$\leq$-3.0). Similarly, we performed the same type of analysis to all-vs-all African populations, particularly

focused in recent populations that have shown human seeking behavior THI, NGY, OGD, KUM (6,130).

Outlier analysis and local adaptation in populations of *Ae. aegypti*

We screened for SNPs showing unusual patterns of genetic variation along the *Ae. aegypti* genome, with the hypothesis that they contribute to the genetic differentiation among populations. To this end, we used the "outlier method" implemented in the PCAdapt R package v4.3.3 (35), which calculates a PCA from SNP data to search for loci that are atypically related to the population structure by decomposing the 'total' genetic variation into 'axes' of genetic variation (*K*) called "principal components" (PCs). PCAdapt further calculates the correlations between SNPs and a specific number (*K*) of retained PCs, so that SNPs showing an excessive relation with the population structure are defined as outliers and suggested to be candidates for local adaptation. We performed this analysis using the 1,530,512 biallelic chromosomal SNPs that were detected in at least 80% of individuals across all populations; this analysis was performed separately for each chromosome. Importantly, we did not impose any population clustering, but estimated the 'optimal *K* axis' running PCAdapt with an excess of K=20 and assigning the 'optimal *K'* based on three different approaches: 1) the Cattell's rule, which keeps PCs that correspond to eigenvalues to the left of the lower straight line in the screeplot (131); 2) the Tracy-Widow test (p-value<0.05), which was applied to the eigenvalues by using the program *twstats* from the EIGENSOFT v 8.0.0 (34,132); and 3) a pairwise comparison of PCs. This analysis led to the optimal K of 6. SNPs significantly correlated to these 6 PCs were identified through the Mahalanobis distance method as implemented in PCAdapt R (35) and the false discovery rate (FDR) of the p-values was calculated using the qvalue R package v2.18.0 (133). Outlier SNPs were extracted with the *get.pc* function of PCAdapt with an expected 5% of false positives (FDR, α=0.05), and their potential structural and/or functional effect was established implementing three tools: the SnpEff v4.3t program (131), the VariantAnnotation R

720 package (135), and the '*annotate*' function from bcftools using an *in-house* R script from a
721 customized AaegL5 genome annotation file (see below).
722
723 To have an unbiased estimate of local adaptation, we established a statistical framework to associate
724 the PC-specific outliers to a population. Briefly, we used the PC scores generated for each mosquito
725 from the covariance matrix of the PCA, and then analyzed their distribution across populations on
726 each of the 6 PCs, separately, as implemented in previous studies (136,137). A PC score represents
727 not only the PCA projections of a single genome, but also an independent measure of variation in
728 the form of values that are different from zero. We used these PC scores to identify members of a
729 population with patterns of high variance to support their local genetic differentiation. We defined
730 a population to be locally differentiated when the distribution of the PC scores significantly departs
731 from zero. This significance was tested by evaluating whether PC scores from a population are
732 significantly different from zero on the corresponding PC (one sample t-test, m=0), and also if they
733 are significantly different from other populations (pairwise t-test). Final candidates were obtained
734 after manually comparing those populations with significant PC scores. To support estimates of
735 local genetic adaptation, we used two additional parameters of genetic diversity: F_{ST} and Tajima's
736 D, which were calculated using VCFTools. The F_{ST} value of each outlier SNP was used as a
737 measurement of the "intensity" of genetic differentiation and Tajima's D was estimated in genes
738 with outlier SNPs to identify whether such genetic variation is different from neutrality ($-0.5 < D$
739 <1.0).
740
741 To identify a set of genes that shows a strong signal of genetic differentiation between Aaa and Aaf,
742 we first identified with a custom PERL program all genes associated with outlier SNPs and
743 quantified their occurrence across genomic regions and effects (*i.e.*, synonymous and non-
744 synonymous mutations). Next, allele frequencies of all non-synonymous SNPs were obtained for
745 each gene across all populations. To evaluate significant differences between Aaa and Aaf

populations in this filtered set of genes, we created 4 groups of populations based on the genetic diversity and divergence patterns we observed in our data: 1) THI and NGY, 2) RABs and RABd, 3) the rest of African populations, and 4) all out of Africa populations. Despite the genetic difference between these groups, our null hypothesis is to find genes significantly differentiated between Aaa and Aaf (Ho), this will be rejected ($p>0.05$) for cases in which no major differences can be detected using an ANOVA test.

A GO enrichment analysis across the three major GO categories (Biological Processes, Molecular Functions, and Cellular Components) was performed to identify functional groups that were enriched in this set of genes. Briefly, we used a custom genome database for *Ae. aegypti* with GO annotations (*in-house* org.Aaegypti.eg.db R package, see below) and the clusterProfiler R package v4.2.2 (138) to calculate the GO enrichment. *P*-values ($p\leq0.05$) were corrected for multiple tests using the Benjamini-Hochberg procedure, and redundancy of enriched GO terms on each major GO classification was removed with the function *simplify*, both implemented in clusterProfiler (135). The custom org.Aaegypti.eg.db R package was built based on a collection of GO annotations retrieved from VectorBase version 59 (139) and a bioinformatic approach using BLAST (NCBI Diptera *non-redundant* (nr) database v5) and InterProScan v5 (140) scanning different protein domain databases: Pfam v33.1 (141), ProSiteProfiles v20.2 (142), SUPERFMILY v2.0 (143), and TIGRFAM v15.0 (144). Outlier SNPs were also mapped against a target set of 1132 genes, including 198 detoxification genes, 198 chemosensory genes (OR, IR and GR receptors), 391 immunity genes, 292 proteases, and 53 genes associated to multiple functions (32,64,65).

Assessing Ka/Ks ratio

We estimated the ratio of non-synonymous (Ka) to synonymous (Ks) substitutions (also known as dN/dS ratio) across 13,503 of the 14,677 *Ae. aegypti* protein coding genes, and identified genes as evolving neutrally or nearly neutral with a conservative threshold of $0.95\geq Ka/Ks\leq1.05$, or under

772 negative selection when Ka/Ks<0.95 (and 0.80≤Ka/Ks<0.95 for weak negative selection), or under
773 positive selection when Ka/Ks>1.05 (and 1.05>Ka/Ks≤1.2 for weak positive selection) (57). A total
774 of 1,174 genes were not analyzed due to either the absence of SNPs and/or the presence of multiples
775 indels affecting the positions of codons. To do this, we first extracted codons associated to SNPs
776 and classified into non-degenerate (L0) sites, 2-fold (L2) degenerated sites, and 4-fold (L4)
777 degenerated sites. Next, transition (Ts) and transversion (Tv) changes were identified for each
778 codon by comparing the alternative and reference alleles and obtaining the number of Ts at L0 (A0),
779 L2 (A2), and L4 (A2) degenerated sites, as well as the number of Tv at L0 (B0), L2 (B2), and L4
780 (B2) degenerated sites. The rates of *Ka* and *Ks* site substitution were calculated using the improved
781 Kimura-2 parameters (K2P) Li's method (145,146).
782
783 We also estimated the ratio of Ka/Ks by gene in each population using the PAML package v4.10.6
784 (147). For this analysis, we derived 539,298 gene nucleotide alignments with the *vcf2fasta* package
785 (https://github.com/santiagosnchez/vcf2fasta) from protein coding genes with at least 1 SNP in each
786 population. Then, each alignment was translated into amino acids sequences with *transeq* from the
787 EMBOSS package v6.6.0.0 (148), and their corresponding codon alignments were created with the
788 *pal2nal.pl* program v14 (149). A total of 162 protein coding genes were removed from this analysis
789 due to the presence of multiples indels affecting the positions of codons, resulting in a final dataset
790 of 539,136 codon alignments. A ML phylogenetic tree was reconstructed for each codon alignment
791 with *FastTree* v2.1 (150) and the GTR+GAMMA model. The *one-ratio model* (M0) was used to
792 calculate the ka/ks ratio average for the whole gene over all branches in the phylogeny with the
793 *codeml* program from the PAML package (147). The Ka/Ks ratio of a gene was the average Ka/Ks
794 ratios calculated within the gene. PAML detected 2.5-fold times more sites under selection than the
795 improved K2P Li's method. However, ~37% of the Ka/Ks ratios detected with PAML exhibit
796 standard deviations >10, suggesting either a high divergence among individuals within a population
797 or an overestimation of the Ka/Ks ratio *per* gene. The latter is more probable because the PAML-

based Ka/Ks ratio method ignores SNPs segregating within a population and transient SNPs within divergent populations (151–153). Based on these results, we further analyzed and discussed only the Ka/Ks ratios estimated with the improved K2P Li's method.

Analysis of *Ae. aegypti* nrEVEs

The frequency of each of the 252 nrEVEs annotated in AaegL5 was established in each of the analyzed populations using the SVD pipeline (46,48,154). The same procedure was used to verify the occurrence of *Ae. aegypti* nrEVEs in 4 WGS dataset from *Ae. mascarensis* (10).

The Vy-PER (155 and ViR (48) pipelines were used to search for novel viral integrations using a viral database assembled in October 2020, which encompasses a total of 1778 taxids and 3677 nucleotide sequences of both DNA and RNA viruses. To build the viral database, viral taxids were extracted from NCBI virus (https://www.ncbi.nlm.nih.gov/labs/virus/vssi/#/) according to three different criteria: (i) main known arboviral genera; (ii) ISVs identified from a search of NCBI PubMed publications between 2015 and 2020 using the keyword 'insect specific viruses'; (iii) viruses having Diptera as host. Nucleotide sequences for the accessions corresponding to the selected taxids were retrieved using the NCBI E-utility tool. After removing duplicates, sequences were clustered at 97% identity using CD-HIT (156). Sequences were BLAST searched against a database of conserved eukaryotic and bacterial ribosomal sequences developed for SortmeRNA (157) and of Diptera ribosomal sequences extracted from (158). Entire sequences or parts of sequences matching ribosomal DNA were removed or masked, respectively. Homopolymers and repeats were identified using a custom script and masked with Ns. The presence of novel nrEVEs was further tested in all WGS data used for SNP discovery using the ViR_LTFinder script (48) to confirm their widespread distribution in African vs out-of-Africa samples. A subset of 26 out of the 64 novel nrEVEs were molecularly validated by PCR and Sanger sequencing in the mosquito DNA samples that had been used for WGS using primers designed on the bioinformatic predictions generated by ViR. PCRs were performed in 50 mL of volume containing 25 mL of 2X DreamTaq

Green PCR Master Mix (ThermoFisher), 2.5 mL of 10 mM forward and reverse primers, 1 mL of DNA diluted 1:10 and sterile water to volume. Reactions without template served as negative controls. PCR products were visualized through electrophoresis on 2% agarose gels stained with ethidium bromide. Since multiple bands were often observed, bands of expected size were cut from the gels and purified using the GeneJET PCR Purification Kit (Thermo Scientific), following the manufacturer's protocol. Purified PCR products were sent for Sanger sequencing to Macrogen Europe (Netherlands) to confirm nrEVE sequence.

This version of the Manuscript has not supplementary material.

References and Notes

1. Andersson L, Purugganan M. Molecular genetic variation of animals and plants under domestication. Proceedings of the National Academy of Sciences. 2022;119(30):e2122150119.
2. Hulme-Beaman A, Orton D, Cucchi T. The origins of the domesticate brown rat (*Rattus norvegicus*) and its pathways to domestication. Animal Frontiers. 2021;11(3).
3. Morand S, McIntyre KM, Baylis M. Domesticated animals and human infectious diseases of zoonotic origins: Domestication time matters. Infection, Genetics and Evolution. 2014;24.
4. Souza-Neto JA, Powell JR, Bonizzoni M. *Aedes aegypti* vector competence studies: A review. Vol. 67, Infection, Genetics and Evolution. 2019.
5. Aubry F, Dabo S, Manet C, Filipović I, Rose NH, Miot EF, et al. Enhanced Zika virus susceptibility of globally invasive *Aedes aegypti* populations. Science (1979). 2020;370(6519).
6. Rose NH, Sylla M, Badolo A, Lutomiah J, Ayala D, Aribodor OB, et al. Climate and Urbanization Drive Mosquito Preference for Humans. Current Biology. 2020;30(18).
7. Mattingly PF. Genetical aspects of the *Aedes aegypti* problem. Ann Trop Med Parasitol. 1957;51(4).
8. Paupy C, Brengues C, Kamgang B, Hervé JP, Fontenille D, Simard F. Gene flow between domestic and sylvan populations of *Aedes aegypti* (Diptera: Culicidae) in North Cameroon. J Med Entomol. 2008;45(3).
9. Sylla M, Bosio C, Urdaneta-Marquez L, Ndiaye M, Black IV WC. Gene flow, subspecies composition, and dengue virus-2 susceptibility among *Aedes aegypti* collections in Senegal. PLoS Negl Trop Dis. 2009;3(4).
10. Soghigian J, Gloria-Soria A, Robert V, le Goff G, Failloux AB, Powell JR. Genetic evidence for the origin of *Aedes aegypti*, the yellow fever mosquito, in the southwestern Indian Ocean. Mol Ecol. 2020;29(19).
11. Powell JR, Tabachnick WJ. History of domestication and spread of *Aedes aegypti*--a review. Vol. 108, Memórias do Instituto Oswaldo Cruz. 2013.
12. Rose NH, Badolo A, Sylla M, Akorli J, Otoo S, Gloria-Soria A, et al. Dating the origin and spread of specialization on human hosts in *Aedes aegypti* mosquitoes. bioRxiv. 2022;2022–9.
13. Crawford JE, Alves JM, Palmer WJ, Day JP, Sylla M, Ramasamy R, et al. Population genomics reveals that an anthropophilic population of *Aedes aegypti* mosquitoes in West Africa recently gave rise to American and Asian populations of this major disease vector. BMC Biol. 2017;15(1).
14. Brown JE, Evans BR, Zheng W, Obas V, Barrera-Martinez L, Egizi A, et al. Human impacts have shaped historical and recent evolution in *Aedes aegypti*, the dengue and yellow fever mosquito. Evolution (N Y). 2014;68(2).
15. Brown JE, Mcbride CS, Johnson P, Ritchie S, Paupy C, Bossin H, et al. Worldwide patterns of genetic differentiation imply multiple 'domestications' of *Aedes aegypti*, a major vector of human diseases. Proceedings of the Royal Society B: Biological Sciences. 2011;278(1717).
16. Gloria-Soria A, Ayala D, Bheecarry A, Calderon-Arguedas O, Chadee DD, Chiappero M, et al. Global genetic diversity of *Aedes aegypti*. Mol Ecol. 2016;25(21).
17. Powell JR, Gloria-Soria A, Kotsakiozi P. Recent history of *Aedes aegypti*: Vector genomics and epidemiology records. Vol. 68, BioScience. 2018.

18. Bennett KL, Shija F, Linton YM, Misinzo G, Kaddumukasa M, Djouaka R, et al. Historical environmental change in Africa drives divergence and admixture of *Aedes aegypti* mosquitoes: a precursor to successful worldwide colonization? Mol Ecol. 2016;25(17).
19. Ayres CFJ, Melo-Santos MAV, Solé-Cava AM, Furtado AF. Genetic differentiation of *Aedes aegypti* (Diptera: Culicidae), the major dengue vector in Brazil. J Med Entomol. 2003;40(4).
20. Suesdek L. Microevolution of medically important mosquitoes – A review. Vol. 191, Acta Tropica. 2019.
21. Redmond SN, Sharma A, Sharakhov I, Tu Z, Sharakhova M, Neafsey DE. Linked-read sequencing identifies abundant microinversions and introgression in the arboviral vector *Aedes aegypti*. BMC Biol. 2020;18(1).
22. Liu N. Insecticide resistance in mosquitoes: Impact, mechanisms, and research directions. Vol. 60, Annual Review of Entomology. 2015.
23. Faucon F, Dusfour I, Gaude T, Navratil V, Boyer F, Chandre F, et al. Identifying genomic changes associated with insecticide resistance in the dengue mosquito *Aedes aegypti* by deep targeted sequencing. Genome Res. 2015;25(9).
24. Moyes CL, Vontas J, Martins AJ, Ng LC, Koou SY, Dusfour I, et al. Contemporary status of insecticide resistance in the major *Aedes* vectors of arboviruses infecting humans. Vol. 11, PLoS Neglected Tropical Diseases. 2017.
25. Nag DK, Dieme C, Lapierre P, Lasek-Nesselquist E, Kramer LD. RNA-Seq analysis of blood meal induced gene-expression changes in Aedes aegypti ovaries. BMC Genomics. 2021;22(1).
26. McBride CS, Baier F, Omondi AB, Spitzer SA, Lutomiah J, Sang R, et al. Evolution of mosquito preference for humans linked to an odorant receptor. Nature. 2014;515(7526).
27. Ni M, Zhao T, Lv H xin, Li M jin, Xing D, Zhao T yan, et al. Screening for odorant receptor genes expressed in *Aedes aegypti* involved in host-seeking, blood-feeding and oviposition behaviors. Parasit Vectors. 2022;15(1).
28. David JP, Ismail HM, Chandor-Proust A, Paine MJI. Role of cytochrome P450s in insecticide resistance: Impact on the control of mosquito-borne diseases and use of insecticides on earth. Vol. 368, Philosophical Transactions of the Royal Society B: Biological Sciences. 2013.
29. Croset V, Rytz R, Cummins SF, Budd A, Brawand D, Kaessmann H, et al. Ancient protostome origin of chemosensory ionotropic glutamate receptors and the evolution of insect taste and olfaction. PLoS Genet. 2010;6(8).
30. Cosme L v, Lima JBP, Powell JR, Martins AJ. Genome-wide Association Study Reveals New Loci Associated with Pyrethroid Resistance in *Aedes aegypti*. Front Genet. 2022;13.
31. Love RR, Sikder JR, Vivero RJ, Matute DR, Schrider DR. Strong positive selection in *Aedes aegypti* and the rapid evolution of insecticide resistance. bioRxiv. 2022;2022–7.
32. Matthews BJ, Dudchenko O, Kingan SB, Koren S, Antoshechkin I, Crawford JE, et al. Improved reference genome of *Aedes aegypti* informs arbovirus vector control. Nature. 2018;563(7732).
33. Pickrell JK, Pritchard JK. Inference of Population Splits and Mixtures from Genome-Wide Allele Frequency Data. PLoS Genet. 2012;8(11).
34. Patterson N, Moorjani P, Luo Y, Mallick S, Rohland N, Zhan Y, et al. Ancient admixture in human history. Genetics. 2012;192(3).
35. Privé F, Luu K, Vilhjálmsson BJ, Blum MGB, Rosenberg M. Performing Highly Efficient Genome Scans for Local Adaptation with R Package pcadapt Version 4. Mol Biol Evol. 2020;37(7).
36. Rose NH, Dabo S, da Veiga Leal S, Sylla M, Diagne CT, Faye O, et al. Enhanced mosquito vectorial capacity underlies the Cape Verde Zika epidemic. PLoS Biol. 2022;20(10):e3001864.
37. Smith LB, Tyagi R, Kasai S, Scott JG. CYP-mediated permethrin resistance in *Aedes aegypti* and evidence for trans-regulation. PLoS Negl Trop Dis. 2018;12(11).
38. Gan SJ, Leong YQ, bin Barhanuddin MFH, Wong ST, Wong SF, Mak JW, et al. Dengue fever and insecticide resistance in *Aedes* mosquitoes in Southeast Asia: a review. Vol. 14, Parasites and Vectors. 2021.
39. Epelboin Y, Wang L, Gianetto QG, Choumet V, Gaborit P, Issaly J, et al. CYP450 core involvement in multiple resistance strains of *Aedes aegypti* from French Guiana highlighted by proteomics, molecular and biochemical studies. PLoS One. 2021;16(1 January).
40. Gereau RW, Swanson G. The glutamate receptors. Springer Science & Business Media; 2008.
41. Hellmich E, Nusawardani T, Bartholomay L, Jurenka R. Pyrokinin/PBAN-like peptides in the central nervous system of mosquitoes. Cell Tissue Res. 2014;356(1).
42. Bader R, Colomb J, Pankratz B, Schröck A, Stocker RF, Pankratz MJ. Genetic dissection of neural circuit anatomy underlying feeding behavior in *Drosophila*: Distinct classes of hugin-expressing neurons. Journal of Comparative Neurology. 2007;502(5).
43. Pollock VP, McGettigan J, Cabrero P, Maudlin IM, Dow JAT, Davies SA. Conservation of capa peptide-induced nitric oxide signaling in Diptera. Journal of Experimental Biology. 2004;207(23).
44. Sauvola CW, Akbergenova Y, Cunningham KL, Aponte-Santiago NA, Troy Littleton J. The decoy snare tomosyn sets tonic versus phasic release properties and is required for homeostatic synaptic plasticity. Elife. 2021;10.
45. Littleton JT, Bellen HJ, Perin MS. Expression of synaptotagmin in *Drosophila* reveals transport and localization of synaptic vesicles to the synapse. Development. 1993;118(4).

46. Dwivedi S, Muthusamy B, Kumar P, Kim MS, Nittujogi RS, et al. Brain proteomics of *Anopheles gambiae*. OMICS A journal of Integrative Biology. 2014;18(7).
47. Crava CM, Varghese FS, Pischedda E, Halbach R, Palatini U, Marconcini M, et al. Population genomics in the arboviral vector *Aedes aegypti* reveals the genomic architecture and evolution of endogenous viral elements. Mol Ecol. 2021;30(7).
48. Suzuki Y, Baidaliuk A, Miesen P, Frangeul L, Crist AB, Merkling SH, et al. Non-retroviral Endogenous Viral Element Limits Cognate Virus Replication in *Aedes aegypti* Ovaries. Current Biology. 2020;30(18).
49. Pischedda E, Crava C, Carlassara M, Zucca S, Gasmi L, Bonizzoni M. ViR: a tool to solve intrasample variability in the prediction of viral integration sites using whole genome sequencing data. BMC Bioinformatics. 2021;22(1).
50. Zhang J, Liu H, Wang J, Wang J, Zhang J, Wang J, et al. Origin and evolution of emerging Liao ning Virus (genus Seadornavirus, family Reoviridae). Virol J. 2020;17(1).
51. Bisch-Knaden S, Daimon T, Shimada T, Hansson BS, Sachse S. Anatomical and functional analysis of domestication effects on the olfactory system of the silkmoth *Bombyx mori*. Proceedings of the Royal Society B: Biological Sciences. 2013;281(1774).
52. Wang Q, Ren X, Liu P, Li J, Lv J, Wang J, et al. Improved genome assembly of Chinese shrimp (*Fenneropenaeus chinensis*) suggests adaptation to the environment during evolution and domestication. Mol Ecol Resour. 2022;22(1).
53. Xia S, Cosme L v, Lutomiah J, Sang R, Ngangue MF, Rahola N, et al. Genetic structure of the mosquito *Aedes aegypti* in local forest and domestic habitats in Gabon and Kenya. Parasit Vectors. 2020;13(1).
54. Khater EIM, Baig F, Kamal HA, Powell JR, Saleh AA. Molecular phylogenetics and population genetics of the dengue vector *Aedes aegypti* from the Arabian peninsula. J Med Entomol. 2021;58(6).
55. Diallo D, Diallo M. Resting behavior of *Aedes aegypti* in southeastern Senegal. Parasit Vectors. 2020;13(1).
56. Hurst LD. The Ka/Ks ratio: Diagnosing the form of sequence evolution. Vol. 18, Trends in Genetics. 2002.
57. Yang Z, Bielawski JR. Statistical methods for detecting molecular adaptation. Vol. 15, Trends in Ecology and Evolution. 2000.
58. Matthews BJ, Younger MA, Vosshall LB. The ion channel ppk301 controls freshwater egg-laying in the mosquito *Aedes aegypti*. Elife. 2019;8.
59. Herre M, Goldman O v, Lu TC, Caballero-Vidal G, Qi Y, Gilbert ZN, et al. Non-canonical odor coding in the mosquito. Cell. 2022;185(17):3104–23.
60. Raji JI, Melo N, Castillo JS, Gonzalez S, Saldana V, Stensmyr MC, et al. *Aedes aegypti* Mosquitoes Detect Acidic Volatiles Found in Human Odor Using the IR8a Pathway. Current Biology. 2019;29(8).
61. de Obaldia ME, Morita T, Dedmon LC, Boehmler DJ, Jiang CS, Zeledon E v, et al. Differential mosquito attraction to humans is associated with skin-derived carboxylic acid levels. Cell. 2022;185(22):4099–116.
62. McMeniman CJ, Corfas RA, Matthews BJ, Ritchie SA, Vosshall LB. Multimodal integration of carbon dioxide and other sensory cues drives mosquito attraction to humans. Cell. 2014;156(5).
63. Sorrells TR, Pandey A, Rosas-Villegas A, Vosshall LB. A persistent behavioral state enables sustained predation of humans by mosquitoes. Elife. 2022;11:e76663.
64. Strode C, Wondji CS, David JP, Hawkes NJ, Lumjuan N, Nelson DR, et al. Genomic analysis of detoxification genes in the mosquito *Aedes aegypti*. Insect Biochem Mol Biol. 2008;38(1).
65. Waterhouse RM, Kriventseva E v, Meister S, Xi Z, Alvarez KS, Bartholomay LC, et al. Evolutionary dynamics of immune-related genes and pathways in disease-vector mosquitoes. Science (1979). 2007;316(5832).
66. Shin SW, Bian G, Raikhel AS. A toll receptor and a cytokine, Toll5A and Spz1C, are involved in toll antifungal immune signaling in the mosquito *Aedes aegypti*. Journal of Biological Chemistry. 2006;281(51).
67. Saucereau Y, Wilson TH, Tang MCK, Moncrieffe MC, Hardwick SW, Chirgadze DY, et al. Structure and dynamics of Toll immunoreceptor activation in the mosquito *Aedes aegypti*. Nat Commun. 2022;13(1):5110.
68. Licciardi S, Loire E, Cardinale E, Gislard M, Dubois E, Cêtre-Sossah C. In vitro shared transcriptomic responses of *Aedes aegypti* to arboviral infections: Example of dengue and Rift Valley fever viruses. Parasit Vectors. 2020;13(1).
69. Juneja P, Ariani C v., Ho YS, Akorli J, Palmer WJ, Pain A, et al. Exome and Transcriptome Sequencing of *Aedes aegypti* Identifies a Locus That Confers Resistance to *Brugia malayi* and Alters the Immune Response. PLoS Pathog. 2015;11(3).
70. Carneiro M, Rubin CJ, Palma F di, Albert FW, Alföldi J, Barrio AM, et al. Rabbit genome analysis reveals a polygenic basis for phenotypic change during domestication. Science (1979). 2014;345(6200).
71. Rubin CJ, Zody MC, Eriksson J, Meadows JRS, Sherwood E, Webster MT, et al. Whole-genome resequencing reveals loci under selection during chicken domestication. Nature. 2010;464(7288).
72. Karlsson AC, Fallahshahroudi A, Johnsen H, Hagenblad J, Wright D, Andersson L, et al. A domestication related mutation in the thyroid stimulating hormone receptor gene (TSHR) modulates photoperiodic response and reproduction in chickens. Gen Comp Endocrinol. 2016;228.
73. Bernhardt SA, Blair C, Sylla M, Bosio C, Black IV WC. Evidence of multiple chromosomal inversions in Aedes aegypti formosus from Senegal. Insect Mol Biol. 2009;18(5).

74. Rottschaefer SM, Riehle MM, Coulibaly B, Sacko M, Niaré O, Morlais I, et al. Exceptional diversity, maintenance of polymorphism, and recent directional selection on the APL1 malaria resistance genes of Anopheles gambiae. PLoS Biol. 2011;9(3).
75. Donnelly MJ, Pinto J, Girod R, Besansky NJ, Lehmann T. Revisiting the role of introgression vs shared ancestral polymorphisms as key processes shaping genetic diversity in the recently separated sibling species of the *Anopheles gambiae* complex. Heredity (Edinb). 2004;92(2).
76. Rottschaefer SM, Riehle MM, Coulibaly B, Sacko M, Niaré O, Morlais I, et al. Exceptional diversity, maintenance of polymorphism, and recent directional selection on the APL1 malaria resistance genes of *Anopheles gambiae*. PLoS Biol. 2011;9(3).
77. Miles A, Harding NJ, Bottà G, Clarkson CS, Antão T, Kozak K, et al. Genetic diversity of the African malaria vector anopheles gambiae. Nature. 2017;552.
78. Wilke ABB, de Carvalho GC, Marrelli MT. Retention of ancestral polymorphism in *Culex nigripalpus* (Diptera: Culicidae) from São Paulo, Brazil. Infection, Genetics and Evolution. 2018;65.
79. Fonseca DM, Smith JL, Wilkerson RC, Fleischer RC. Pathways of expansion and multiple introductions illustrated by large genetic differentiation among worldwide populations of the southern house mosquito. American Journal of Tropical Medicine and Hygiene. 2006;74(2).
80. Barrett RDH, Schluter D. Adaptation from standing genetic variation. Trends Ecol Evol. 2008;23(1):38–44.
81. Chaturvedi A, Zhou J, Raeymaekers JAM, Czypionka T, Orsini L, Jackson CE, et al. Extensive standing genetic variation from a small number of founders enables rapid adaptation in *Daphnia*. Nat Commun. 2021;12(1).
82. Jones FC, Grabherr MG, Chan YF, Russell P, Mauceli E, Johnson J, et al. The genomic basis of adaptive evolution in threespine sticklebacks. Nature. 2012;484(7392).
83. Reid NM, Proestou DA, Clark BW, Warren WC, Colbourne JK, Shaw JR, et al. The genomic landscape of rapid repeated evolutionary adaptation to toxic pollution in wild fish. Science (1979). 2016;354(6317).
84. Lai YT, Yeung CKL, Omland KE, Pang EL, Hao Y, Liao BY, et al. Standing genetic variation as the predominant source for adaptation of a songbird. Proc Natl Acad Sci U S A. 2019;116(6).
85. McCoy RC, Akey JM. Selection plays the hand it was dealt: Evidence that human adaptation commonly targets standing genetic variation. Genome Biol. 2017;18(1).
86. Leming MT, Rund SSC, Behura SK, Duffield GE, O'Tousa JE. A database of circadian and diel rhythmic gene expression in the yellow fever mosquito *Aedes aegypti*. BMC Genomics. 2014;15(1).
87. Li X, Yang J, Pu Q, Peng X, Xu L, Liu S. Serine hydroxymethyltransferase controls blood-meal digestion in the midgut of Aedes aegypti mosquitoes. Parasit Vectors. 2019;12(1).
88. Hixson B, Bing XL, Yang X, Bonfini A, Nagy P, Buchon N. A transcriptomic atlas of *Aedes aegypti* reveals detailed functional organization of major body parts and gut regional specializations in sugar-fed and blood-fed adult females. Elife. 2022;11:e76132.
89. Riabinina O, Task D, Marr E, Lin CC, Alford R, O'Brochta DA, et al. Organization of olfactory centers in the malaria mosquito *Anopheles gambiae*. Nat Commun. 2016;7.
90. Kokoza VA, Raikhel AS. Targeted gene expression in the transgenic *Aedes aegypti* using the binary Gal4-UAS system. Insect Biochem Mol Biol. 2011;41(8).
91. Kistler KE, Vosshall LB, Matthews BJ. Genome engineering with CRISPR-Cas9 in the mosquito *Aedes aegypti*. Cell Rep. 2015;11(1).
92. Zhao Z, Tian D, McBride CS. Development of a pan-neuronal genetic driver in *Aedes aegypti* mosquitoes. Cell Reports Methods. 2021;1(3).
93. Marconcini M, Pischedda E, Houé V, Palatini U, Lozada-Chávez N, Sogliani D, et al. Profile of small RNAs, vDNA forms and viral integrations in late chikungunya virus infection of *Aedes albopictus* mosquitoes. Viruses. 2021;13(4).
94. Andrews S. FastQC - A quality control tool for high throughput sequence data. http://www.bioinformatics.babraham.ac.uk/projects/fastqc/. Babraham Bioinformatics. 2010;
95. Bolger AM, Lohse M, Usadel B. Trimmomatic: A flexible trimmer for Illumina sequence data. Bioinformatics. 2014;30(15).
96. Palatini U, Masri RA, Cosme L v., Koren S, Thibaud-Nissen F, Biedler JK, et al. Improved reference genome of the arboviral vector *Aedes albopictus*. Genome Biol. 2020;21(1).
97. Li H, Durbin R. Fast and accurate long-read alignment with Burrows-Wheeler transform. Bioinformatics. 2010;26(5).
98. Okonechnikov K, Conesa A, García-Alcalde F. Qualimap 2: Advanced multi-sample quality control for high-throughput sequencing data. Bioinformatics. 2016;32(2).
99. Barnett DW, Garrison EK, Quinlan AR, Stŕmberg MP, Marth GT. Bamtools: A C++ API and toolkit for analyzing and managing BAM files. Bioinformatics. 2011;27(12).
100. Pedersen BS, Quinlan AR. Mosdepth: Quick coverage calculation for genomes and exomes. Bioinformatics. 2018;34(5).
101. Aryan A, Anderson MAE, Biedler JK, Qi Y, Overcash JM, Naumenko AN, et al. Nix alone is sufficient to convert female *Aedes aegypti* into fertile males and myo-sex is needed for male flight. Proc Natl Acad Sci U S A. 2020;117(30).

102. Danecek P, Bonfield JK, Liddle J, Marshall J, Ohan V, Pollard MO, et al. Twelve years of SAMtools and BCFtools. Gigascience. 2021;10(2).
103. Depristo MA, Banks E, Poplin R, Garimella K v, Maguire JR, Hartl C, et al. A framework for variation discovery and genotyping using next-generation DNA sequencing data. Nat Genet. 2011;43(5).
104. van der Auwera GA, Carneiro MO, Hartl C, Poplin R, del Angel G, Levy-Moonshine A, et al. From fastQ data to high-confidence variant calls: The genome analysis toolkit best practices pipeline. Curr Protoc Bioinformatics. 2013;(SUPL.43).
105. McKenna A, Hanna M, Banks E, Sivachenko A, Cibulskis K, Kernytsky A, et al. The Genome Analysis Toolkit: a MapReduce framework for analyzing next-generation DNA sequencing data. Genome Res. 2010;20(9):1297–303.
106. Evans BR, Gloria-Soria A, Hou L, McBride C, Bonizzoni M, Zhao H, et al. A multipurpose, high-throughput single-nucleotide polymorphism chip for the dengue and yellow fever mosquito, *Aedes aegypti*. G3: Genes, Genomes, Genetics. 2015;5(5).
107. Saarman NP, Gloria-Soria A, Anderson EC, Evans BR, Pless E, Cosme L v, et al. Effective population sizes of a major vector of human diseases, *Aedes aegypti*. Evol Appl. 2017;10(10).
108. Gloria-Soria A, Lima A, Lovin DD, Cunningham JM, Severson DW, Powell JR. Origin of a high-latitude population of *Aedes aegypti* in Washington, DC. American Journal of Tropical Medicine and Hygiene. 2018;98(2).
109. Kotsakiozi P, Gloria-Soria A, Schaffner F, Robert V, Powell JR. *Aedes aegypti* in the Black Sea: Recent introduction or ancient remnant? Parasit Vectors. 2018;11(1).
110. Kotsakiozi P, Evans BR, Gloria-Soria A, Kamgang B, Mayanja M, Lutwama J, et al. Population structure of a vector of human diseases: *Aedes aegypti* in its ancestral range, Africa. Ecol Evol. 2018;8(16):7835–48.
111. Bonizzoni M, Britton M, Marinotti O, Dunn WA, Fass J, James AA. Probing functional polymorphisms in the dengue vector, Aedes aegypti. BMC Genomics. 2013;14(1).
112. David JP, Faucon F, Chandor-Proust A, Poupardin R, Riaz MA, Bonin A, et al. Comparative analysis of response to selection with three insecticides in the dengue mosquito *Aedes aegypti* using mRNA sequencing. BMC Genomics. 2014;15(1).
113. Pless E, Gloria-Soria A, Evans BR, Kramer V, Bolling BG, Tabachnick WJ, et al. Multiple introductions of the dengue vector, *Aedes aegypti*, into California. PLoS Negl Trop Dis. 2017;11(8).
114. Pracana R, Priyam A, Levantis I, Nichols RA, Wurm Y. The fire ant social chromosome supergene variant Sb shows low diversity but high divergence from SB. Mol Ecol. 2017;26(11).
115. Kent WJ, Baertsch R, Hinrichs A, Miller W, Haussler D. Evolution's cauldron: Duplication, deletion, and rearrangement in the mouse and human genomes. Proc Natl Acad Sci U S A. 2003;100(20).
116. Gremme G, Steinbiss S, Kurtz S. Genome tools: A comprehensive software library for efficient processing of structured genome annotations. IEEE/ACM Trans Comput Biol Bioinform. 2013;10(3).
117. Kent WJ. BLAT - The BLAST-like alignment tool. Genome Res. 2002;12(4).
118. Wang M, Kong L. pblat: A multithread blat algorithm speeding up aligning sequences to genomes. BMC Bioinformatics. 2019;20(1).
119. Zhao H, Sun Z, Wang J, Huang H, Kocher JP, Wang L. CrossMap: A versatile tool for coordinate conversion between genome assemblies. Bioinformatics. 2014;30(7).
120. Bian X, Zhu B, Wang M, Hu Y, Chen Q, Nguyen C, et al. Comparing the performance of selected variant callers using synthetic data and genome segmentation. BMC Bioinformatics. 2018;19(1).
121. Kumaran M, Subramanian U, Devarajan B. Performance assessment of variant calling pipelines using human whole exome sequencing and simulated data. BMC Bioinformatics. 2019;20(1).
122. Schilbert HM, Rempel A, Pucker B. Comparison of read mapping and variant calling tools for the analysis of plant NGS data. Plants. 2020;9(4).
123. Liu X, Han S, Wang Z, Gelernter J, Yang BZ. Variant Callers for Next-Generation Sequencing Data: A Comparison Study. PLoS One. 2013;8(9).
124. Zheng X, Levine D, Shen J, Gogarten SM, Laurie C, Weir BS. A high-performance computing toolset for relatedness and principal component analysis of SNP data. Bioinformatics. 2012;28(24).
125. Danecek P, Auton A, Abecasis G, Albers CA, Banks E, DePristo MA, et al. The variant call format and VCFtools. Bioinformatics. 2011;27(15):2156–8.
126. Graffelman J, Weir BS. Testing for Hardy-Weinberg equilibrium at biallelic genetic markers on the X chromosome. Heredity (Edinb). 2016;116(6).
127. Alexander DH, Novembre J, Lange K. Fast model-based estimation of ancestry in unrelated individuals. Genome Res. 2009;19(9).
128. Liu CC, Shringarpure S, Lange K, Novembre J. Exploring population structure with admixture models and principal component analysis. In: Methods in Molecular Biology. 2020.
129. Suzuki R, Shimodaira H. Pvclust: An R package for assessing the uncertainty in hierarchical clustering. Bioinformatics. 2006;22(12).
130. Rose NH, Badolo A, Sylla M, Akorli J, Otoo S, Gloria-Soria A, et al. Dating the origin and spread of specialization on human hosts in *Aedes aegypti* mosquitoes. bioRxiv. 2022;2022–9.
131. Cattell RB. The scree test for the number of factors. Multivariate Behav Res. 1966;1(2).

132. Price AL, Patterson NJ, Plenge RM, Weinblatt ME, Shadick NA, Reich D. Principal components analysis corrects for stratification in genome-wide association studies. Nat Genet. 2006;38(8).
133. Dabney A, Storey JD, Warnes GR. qvalue: Q-value estimation for false discovery rate control. R package version. 2010;1(0).
134. Cingolani P, Platts A, Wang LL, Coon M, Nguyen T, Wang L, et al. A program for annotating and predicting the effects of single nucleotide polymorphisms, SnpEff: SNPs in the genome of Drosophila melanogaster strain w1118; iso-2; iso-3. Fly (Austin). 2012;6(2).
135. Obenchain V, Lawrence M, Carey V, Gogarten S, Shannon P, Morgan M. VariantAnnotation: A Bioconductor package for exploration and annotation of genetic variants. Bioinformatics. 2014;30(14).
136. Hickner P v., Timoshevskaya N, Nowling RJ, Labbé F, Nguyen AD, McDowell MA, et al. Molecular signatures of sexual communication in the phlebotomine sand flies. PLoS Negl Trop Dis. 2020;14(12).
137. le Corre V, Siol M, Vigouroux Y, Tenaillon MI, Délye C. Adaptive introgression from maize has facilitated the establishment of teosinte as a noxious weed in Europe. Proc Natl Acad Sci U S A. 2020;117(41).
138. Wu T, Hu E, Xu S, Chen M, Guo P, Dai Z, et al. clusterProfiler 4.0: A universal enrichment tool for interpreting omics data. The Innovation. 2021;2(3).
139. Amos B, Aurrecoechea C, Barba M, Barreto A, Basenko EY, Bażant W, et al. VEuPathDB: The eukaryotic pathogen, vector and host bioinformatics resource center. Nucleic Acids Res. 2022;50(D1).
140. Jones P, Binns D, Chang HY, Fraser M, Li W, McAnulla C, et al. InterProScan 5: Genome-scale protein function classification. Bioinformatics. 2014;30(9).
141. Mistry J, Chuguransky S, Williams L, Qureshi M, Salazar GA, Sonnhammer ELL, et al. Pfam: The protein families database in 2021. Nucleic Acids Res. 2021;49(D1).
142. Sigrist CJA, de Castro E, Cerutti L, Cuche BA, Hulo N, Bridge A, et al. New and continuing developments at PROSITE. Nucleic Acids Res. 2013;41(D1).
143. Wilson D, Pethica R, Zhou Y, Talbot C, Vogel C, Madera M, et al., SUPERFAMILY – Comparative genomics, datamining and sophisticated visualization. Nucleic Acids Res. 2009;D380-6.
144. Haft DH, Selengut JD, White O. The TIGRFAMs database of protein families. Vol. 31, Nucleic Acids Research. 2003.
145. Pamilo P, Bianchi NO. Evolution of the Zfx and Zfy genes: Rates and interdependence between the genes. Mol Biol Evol. 1993;10(2).
146. Li WH. Unbiased estimation of the rates of synonymous and nonsynonymous substitution. J Mol Evol. 1993;36:96–9.
147. Yang Z. PAML 4: Phylogenetic analysis by maximum likelihood. Mol Biol Evol. 2007;24(8).
148. Rice P, Longden I, Bleasby A. EMBOSS: the European molecular biology open software suite. Trends Genet. 2000;16:276-277.
149. Suyama M, Torrents D, Bork P. PAL2NAL: robust conversion of protein sequence alignments into the corresponding codon alignments. Nucleic Acids Res. 2006;34:W609-12.
150. Price MN, Dehal PS, Arkin AP. FastTree2- Approximately Maximum-Likelihood Trees for large Alignments. PLoS One 2010;5(3):e9490.
151. Zhang J, Nielsen R, Yang Z. Evaluation of an improved branch-site likelihood method for detecting positive selection at the molecular level. Mol Biol Evol. 2005;22(12).
152. Wong WSW, Yang Z, Goldman N, Nielsen R. Accuracy and power of statistical methods for detecting adaptive evolution in protein coding sequences and for identifying positively selected sites. Genetics. 2004;168(2).
153. Kryazhimskiy S, Plotkin JB. The population genetics of dN/dS. PLoS Genet. 2008;4(12).
154. Palatini U, Pischedda E, Bonizzoni M. Computational methods for the discovery and annotation of viral integrations. In: piRNA: Methods and Protocols. Springer; 2022. p. 293–313.
155. Forster M, Szymczak S, Ellinghaus D, Hemmrich G, Rühlemann M, Kraemer L, et al. Vy-PER: Eliminating false positive detection of virus integration events in next generation sequencing data. Sci Rep. 2015;5.
156. Fu L, Niu B, Zhu Z, Wu S, Li W. CD-HIT: Accelerated for clustering the next-generation sequencing data. Bioinformatics. 2012;28(23).
157. Kopylova E, Noé L, Touzet H. SortMeRNA: Fast and accurate filtering of ribosomal RNAs in metatranscriptomic data. Bioinformatics. 2012;28(24).
158. Quast C, Pruesse E, Yilmaz P, Gerken J, Schweer T, Yarza P, et al. The SILVA ribosomal RNA gene database project: Improved data processing and web-based tools. Nucleic Acids Res. 2013;41(D1).

Declarations

Ethics approval and consent to participate: Not applicable

Consent for publication: Not applicable

Data and materials availability: main text or the supplementary materials include all data and information on data accessibility.

Competing interests: authors declare no competing interests.

Funding: the authors would like to thank the following for their financial support of research: Human Frontiers Science Foundation (Research Grant number RGP0007/2017) to M. Bonizzoni and J. Souza-Neto; Italian Ministry of Education, University and Research (FARE-MIUR project R1623HZAH5) to M. Bonizzoni and EU funding within the NextGeneration EU-MUR PNRR Extended Partnership initiative on Emerging Infectious Diseases (Project no. PE00000007, INF-ACT). Sao Paulo Research Foundation Young Investigator Award to J. A. Souza-Neto (Project no. 2013/11343-6).

Author contributions: conceptualization and resources: A. Lozada-Chavez and M. Bonizzoni; whole-genome sequencing: J.A. Souza-Neto, B.C. Carlos and M. Bonizzoni; SNPs identification, population structure and genome-wide codon selection analyses: A. Lozada- Chávez and I. Lozada-Chávez; identification and analyses of nrEVEs: U. Palatini, N. Alfano and M. Bonizzoni; molecular biology data: D. Sogliani and N. Alfano; samples acquisition: T. Degefa, M.V. Sharakhova, A. Badolo, J. Prachumsri, M. Casas-Martinez, B.C. Carlos, L. Lambrechts, J.A. Souza-Neto; figures preparation: A. Lozada- Chávez; N. Alfano; D. Sogliani, U. Palatini; manuscript writing team: A. Lozada-Chávez, I. Lozada-Chávez, S. Elfekih, T. Degefa, M.V. Sharakhova, A. Badolo, J. Prachumsri, M. Casas-Martinez, B. C. Carlos, L. Lambrechts, J.A. Souza-Neto and M. Bonizzoni.

Acknowledgements: We would like to thank members of the Bonizzoni's lab. for fruitful discussion. We thank the members of the Department of Zoonosis and Vector Control from the Municipality of Bebedouro (Brazil) for assistance with mosquito collections.

Figure legends

Fig. 1 Worldwide population structure of African and out-of-Africa samples of *Aedes aegypti*. (**A**) Map of worldwide collection sites of *Aedes aegypti* populations used in this study. Sites are color-coded by region, indicating the sampled regions and the number of their position according to Table 1. (**B**) A Principal Component Analyses (PCA) generated with a panel of 1.5 million of non-redundant and biallelic SNPs from the initial dataset of 634 samples. Each dot represents an individual being color-coded by country (filled circles) and continent (different symbols). Samples from RAB (Kenya) are distinguished as RABd (black solid outlined circles) and RABs (black dotted outlined circles), whereas samples from NGY (Senegal) are divided by showing a strong affinity to Out-of-Africa (blue solid outlined circles) or Western African populations (blue dotted outlined circles). (**C**) ADMIXTURE analyses of population structure for all sampled populations with k=13. On the Y-axis, each vertical bar represents the probability (Q-values from 0 to 1) of assignment of a single individual to each genetic cluster, and each population is separated by a vertical white line and colored according to the legend at the bottom. Individuals with mixed ancestry are denoted by bars with different colors. On the X-axis, country names and numbers are reported according to the abbreviation described in Table 1. African populations were ordered based on their geographical location (Western, Central, and Eastern), and Out of Africa by their corresponding continent. Based on their primary ancestry assignments, African populations are grouped in four genetic clusters: Western (THI and NGY, cluster 2), Western-Central (cluster 5), Central (cluster 3), and Eastern (cluster 4) Africa.

Fig. 2. Evolutionary relationships among 554 *Ae. aegypti* genomes from 39 worldwide populations. (A) A maximum likelihood (ML) tree for individuals including 554 mosquitoes, after 1,000 bootstraps resampling of the dataset. RABd is colored in purple and bold font. THI and NGY mosquitoes are colored in black and bold font. Bootstraps support for each relationship, as well as the geographical region of sampling for each individual, are color-coded accordingly to their symbology. Filled black circles at the base of each individual name are denoting Africa individuals, while open dark circles represent out-of-Africa mosquitoes. **(B)** Divergence among populations based on weighted Fst-based genetic distances, according to the Weir and Cockerham approach. The heatmap is showing a *complete* hierarchical clustering of Fst values from pairwise comparisons across all populations, by using a *euclidean* distance and 1,000 bootstrap replicates. On both axes, population names are shown according to the abbreviation listed on Table 1, with populations clustered and colored by country (Y-axis) and geographical region (X-axis). The diagonal in the matrix represents the comparison with the same population (zero difference, in black), while the degree of divergence for each comparison is shown according to the color symbology at the right bottom. (**C**) A ML tree for populations reconstructed using the same SNPs dataset of tree of individuals but estimating SNPs allele frequencies after 1,000 bootstraps resampling of the dataset. *Ae. albopictus* was used in both ML-trees as an outgroup, and branch lengths in both ML-tress are proportional to the amount of genetic divergence that has occurred.

Fig. 3. Genomic signatures of local adaptation. (**A**) Distribution of the PC scores estimated from outlier SNPs across the three chromosomes of *Ae. aegypti*. On each chromosome panel, the PC scores for each population (on the X-axis) are shown for PC1, PC2, and PC3 (on the Y-axis). Each PC highlights different genomic variants associated to local adaptation in Aaa populations relative to their Aaf counterparts. Each boxplot depicts the variation of the data in a population, indicating the first quantile, mean, third quantile, and the lower and upper whiskers as minimum and maximum

variation of the data population, respectively. PC scores equal to zero are denoted with a horizontal dotted red line. Population names are reported according to their abbreviation in Table 1. (**B**) Distribution of 2,266 protein-coding genes across the *Ae. aegypti* genome that are harboring at least one of the genomic variants detected in (A). The 2,266 genes estimated as locally adapted were plotted for each PC and panel chromosome (1 in left; 2 in central; 3 in right). Chromosomes are depicted as horizontal bars, with locally adapted genes denoted as vertical lines, the frequency of outlier SNPs that each gene harbor is represented by a color gradient according to the symbology. Approximate genomic positions for each chromosome are shown at the bottom.

Fig. 4. Molecular markers differentiating Aaa and Aaf mosquitoes. Box plots depicting the alleles frequencies (on the Y-axis) of nonsynonymous mutations depicted as resulting amino acid change (on X-axis) within selected "*Aaa molecular signature*" genes. Populations are divided and color-coded in four groups, one for all out-of-Africa mosquitoes and three groups for African mosquitoes: Western Senegal (THI-NGY), RABd, Africa (others). (**A**) Examples of genes with known function in chemosensation (Or91, Or86, Ir41, Ir7g, Ir8, Gr9) and immunity (Toll5A, GNBPA2; CLIP12, CLIP8) are shown in separate panels. (**B**) Examples of genes with unknown functions (AAEL025393, AAEL001559, AAEL020878, AAEL022804, AAEL022666, AAEL019451, AAEL012825, AAEL012783, AAEL012268, AAEL010998, AAEL008698). The red dotted line shows the middle value (0.50) of the allele frequency in which all values are distributed.

Fig. 5. Identification of protein-coding selection and *"Aaa molecular signature"* from >13,500 genes in *Ae. aegypti*. The heatmaps in the top panels show the clustering of genes under positive (A) or negative (B) selection in at least one population. Ka/Ks ratio values of A and B were

transformed in a binary matrix based on the Ka/Ks thresholds (see below) defining the *presence* or *absence* of selection acting on genes (on the Y-axis) across Aaf and Aaa populations (on the X-axis), separately. (**A**) When Ka is much greater than Ks (*i.e.*, Ka/Ks >>1) (56), we found 5,242 genes as evolving under positive selection, *i.e.*, their variants are likely beneficial and being promoted. (**B**) When Ka is much less than Ks (*i.e.*, Ka/Ks << 1) (56), then 12,991 genes were estimated as evolving under negative selection, *i.e.*, their variants are likely deleterious and being eliminated. (**C**) The central circle of this polar plot shows the distribution of 419 genes evolving under positive selection (in red-color scale) in at least one population as selected from a catalogue of 1,132 genes belonging to one of the six major functional categories considered relevant for domestication in *Ae. aegypti*. All 40 populations analyzed, 32 from Africa and 8 from out-of-Africa, are located over the Y-axis, while the 419 genes are located over the X-axis. The outer circle shows the cumulative frequency (in bars) of each gene selected positively across the 40 populations, according to the functional category it belongs to as in the legend.

Table 1. (should be added to page 5, line 121)

List of the *Aedes aegypti* populations analyzed, including the number of sequenced genomes (Nr. samples), the total number of SNPs identified (Nr. SNPs), the percentage of variation across the genome and the number of singletons.

Nr.	Continent	Location	Country (Acronym)	Population	Acronym	Nr. Samples	Nr. SNPs	nome variation_	Singletons
1	Africa	Western_Africa	Senegal (SEN)	Bantata	BAN	11	50,915,637	3.98	16,194,719
2				Kedougou	KEN	19	62,102,819	4.86	17,812,101
3				Mindin	MIN	19	61,835,584	4.84	17,319,911
4				Ngoye	NGY	19	53,512,353	4.18	12,022,034
5				PK10	PK10	17	59,791,110	4.68	17,413,512
6				Thiès	THI	11	46,203,180	3.61	11,642,221
7			Burkina_Faso (BFA)	Dori	DOR	14	52,829,396	4.13	15,438,922
8				Ouagadougou	OGD	19	56,323,619	4.40	12,872,274
9				Ouahigouya	OHI	16	57,293,151	4.48	15,994,878
10			Ghana (GHA)	Larabanga	LRB	13	52,202,429	4.08	15,904,999
11				BoabengFiema	BBF	2	16,599,457	1.30	10,985,786
12				Kintampo	KIN	19	60,694,927	4.75	15,965,774
13				Kumasi	KUM	20	59,896,221	4.68	14,516,591
14			Nigeria (NIG)	Awka	AWK	19	61,031,081	4.77	15,951,307
15		Central_Africa	Cameroon (CAM)	Bénoué	BEN	10	37,474,493	2.93	8,832,296
16			Gabon (GAB)	Franceville	FRV	28	64,094,393	5.01	13,413,936
17				Libreville	LBV	12	48,299,015	3.78	11,557,858
18				LopeVillage	LPV	14	54,778,534	4.28	14,789,053
19		Eastern_Africa	Uganda (UGA)	Bundibugyo	BDB	3	24,569,478	1.92	11,952,216
20				Entebbe	ENT	8	44,961,217	3.52	15,676,414
21				Karenga	KRG	3	23,972,914	1.87	10,894,177
22				Kichwamba	KIG	3	25,528,733	2.00	13,356,934
23		Eastern_Africa	Kenya (KEN)	Virhembe	VIR	10	51,812,827	4.05	18,162,017
24				Kakamega	KKM	12	56,512,255	4.42	18,743,667
25				M'barakani village	MBK	15	62,753,159	4.91	21,733,493
26				Ganda	GND	8	49,216,282	3.85	19,458,170
27				Arabuko	ARA	19	69,214,993	5.41	22,091,234
28				KayaBomu	KYB	14	61,448,172	4.81	20,522,089
29				Kwale	KWA	19	68,038,422	5.32	21,472,110
30				ShimbaHills	SHH	7	45,111,490	3.53	18,815,962
31				Rabai	RAB	34	70,217,700	5.49	19,573,051
				Sylvatic		15	65,369,724	5.11	10,612,053
				Domesticated		19	31,131,199	2.43	26,775,337
32	Americas	North_America	Mexico (MEX)	Tapachula	TAP	16	22,994,712	1.80	2,545,413
33		South_America	Brazil (BRZ)	Bebedouro	BEB	12	27,735,391	2.17	3,483,460
34				Santarem	SAN	18	27,688,035	2.17	1,830,877
35	Asia	Western_Asia	Saudi Arabia (SAA)	Jeddah	JED	9	24,610,505	1.92	4,382,323
36		Southeastern_Asia	Thailand (THA)	Samut Sakhon	SAS	16	26,403,048	2.06	3,524,705
37				Bangkok	BNK	19	27,461,673	2.15	2,517,081
38	Oceania	Oceania	American Samoa (AMS)	Tafuna Village	TFV	15	23,464,111	1.83	2,429,934
39			New Caledonia (NCA)	Zac Panda	ZAP	12	26,365,057	2.06	3,033,466

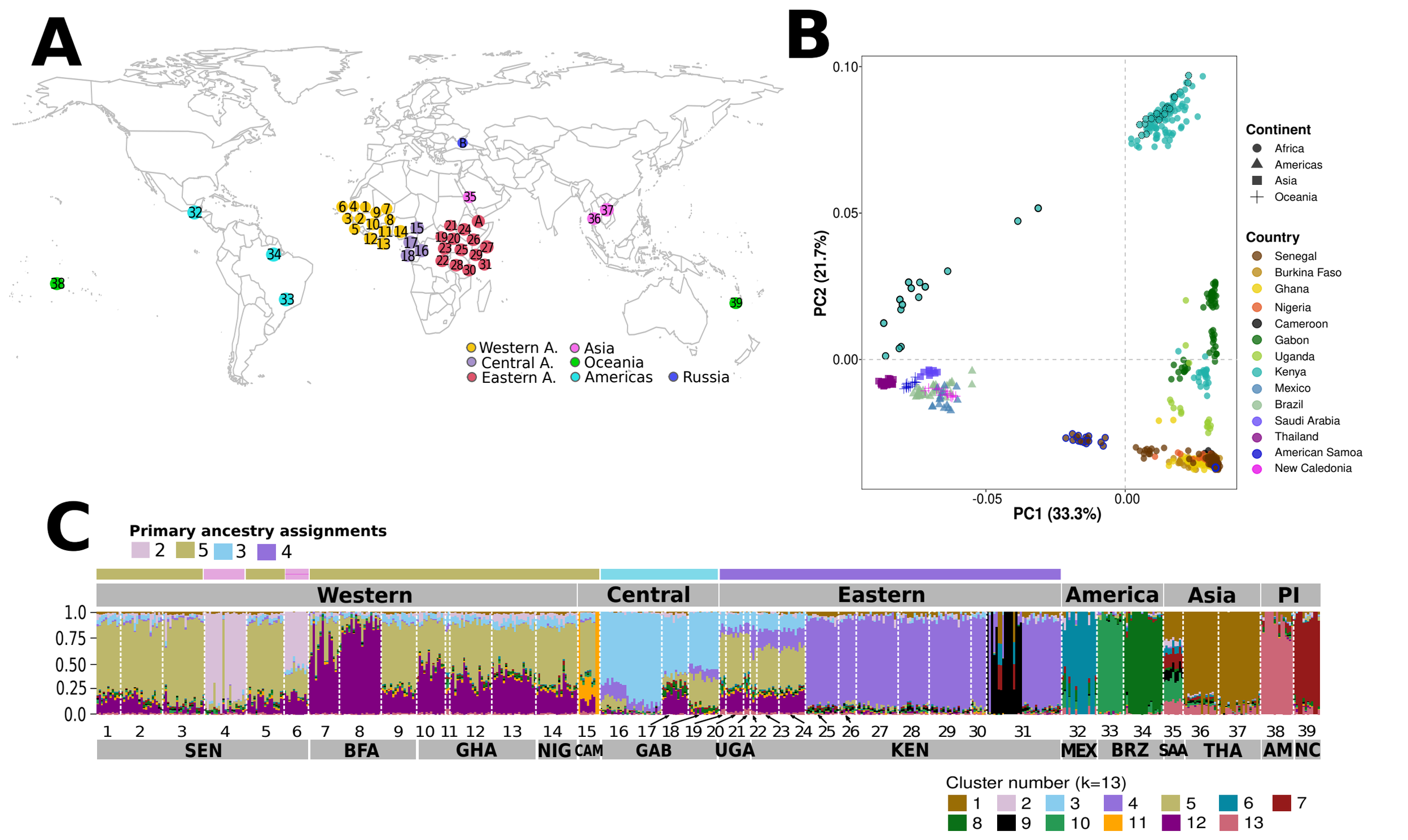
A
Western A.
Central A.
Eastern A.
Asia
Oceania
Americas
Russia
B
PC2 (21.7%)
PC1 (33.3%)
0.10
0.05
0.00
-0.05
0.00
Continent
Africa
Americas
Asia
Oceania
Country
Senegal
Burkina Faso
Ghana
Nigeria
Cameroon
Gabon
Uganda
Kenya
Mexico
Brazil
Saudi Arabia
Thailand
American Samoa
New Caledonia
C
Primary ancestry assignments
2
5
3
4
Western
Central
Eastern
America
Asia
PI
1.0
0.75
0.50
0.25
0.0
SEN
BFA
GHA
NIG
CAM
GAB
UGA
KEN
MEX
BRZ
SAA
THA
AM
NC
Cluster number (k=13)
1
2
3
4
5
6
7
8
9
10
11
12
13

A

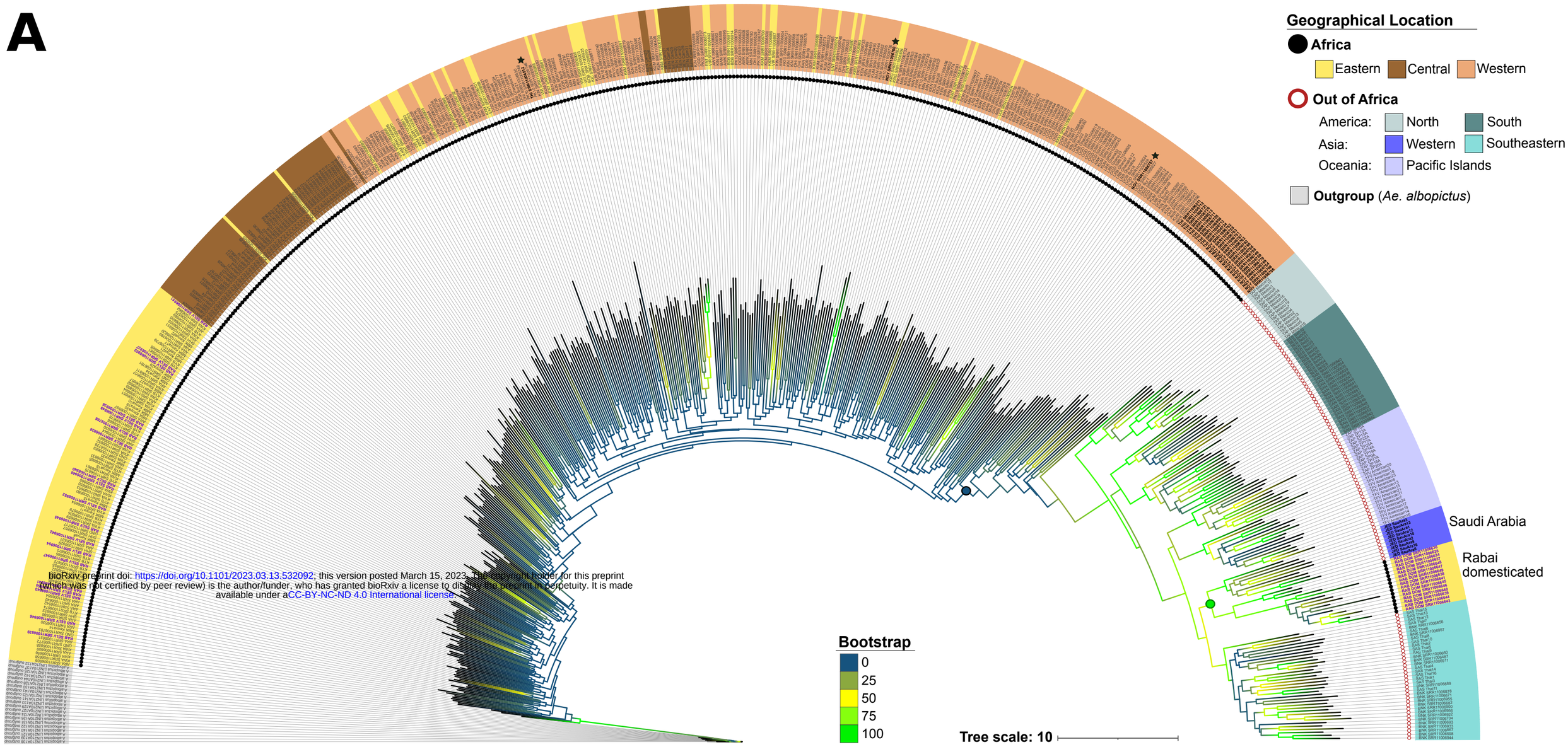

B

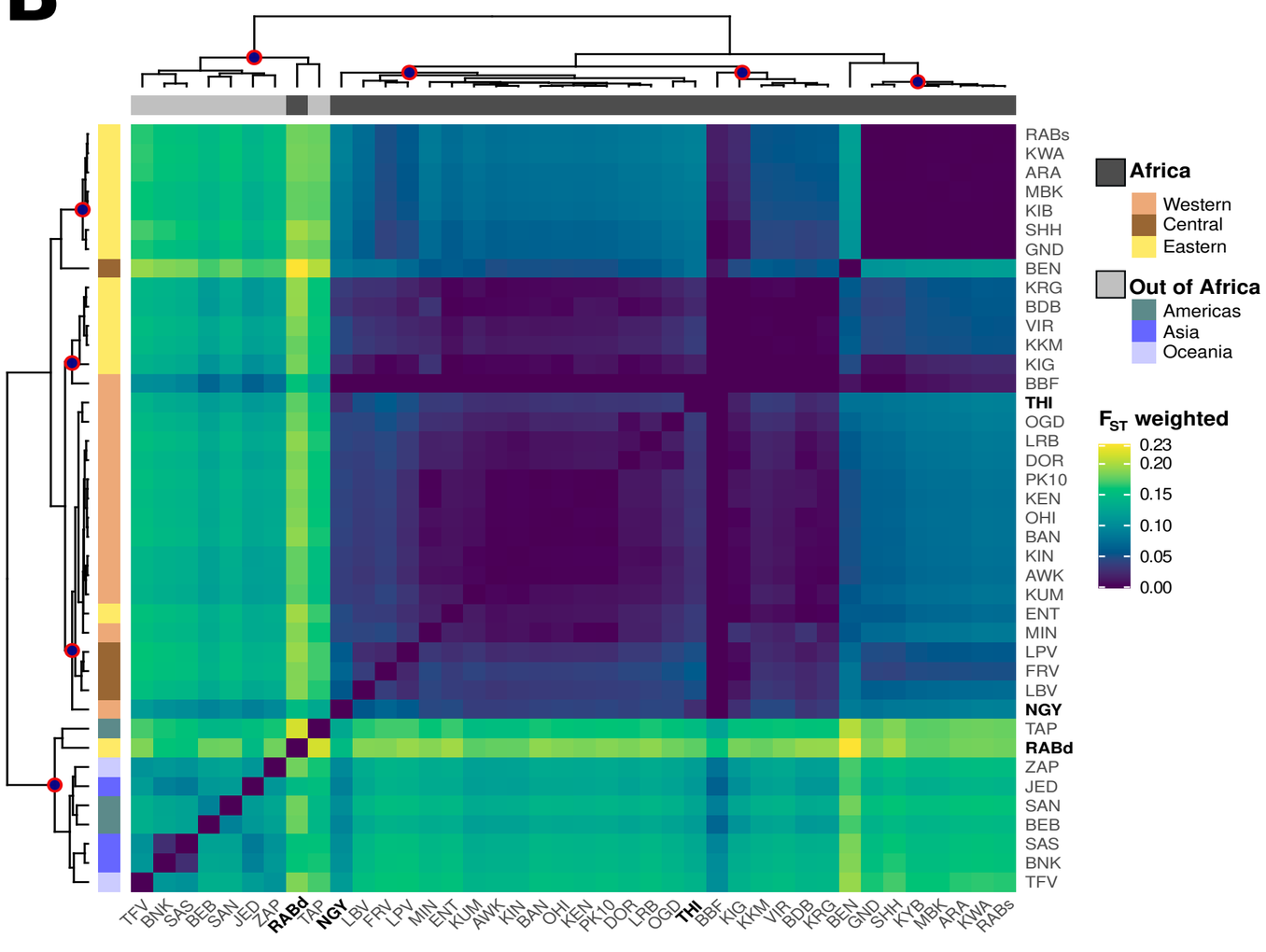

C

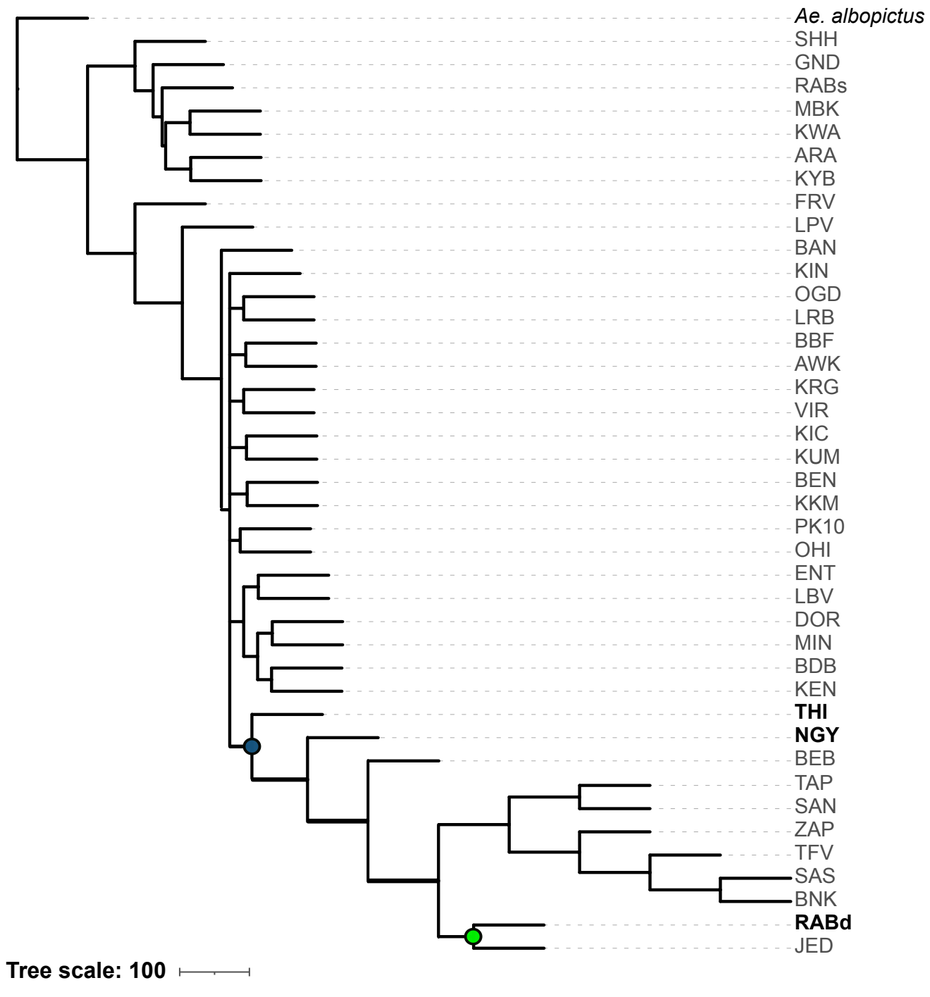

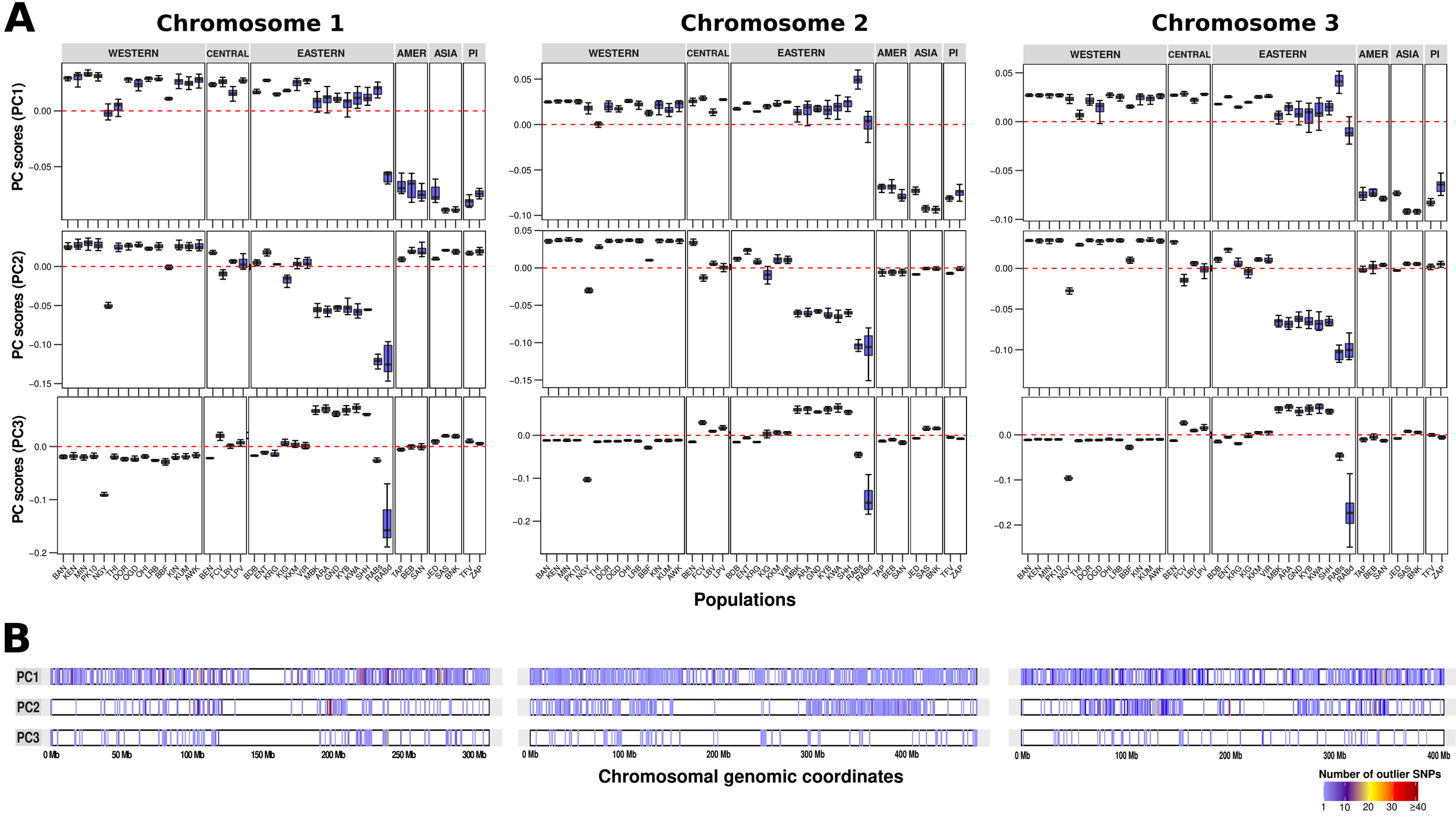

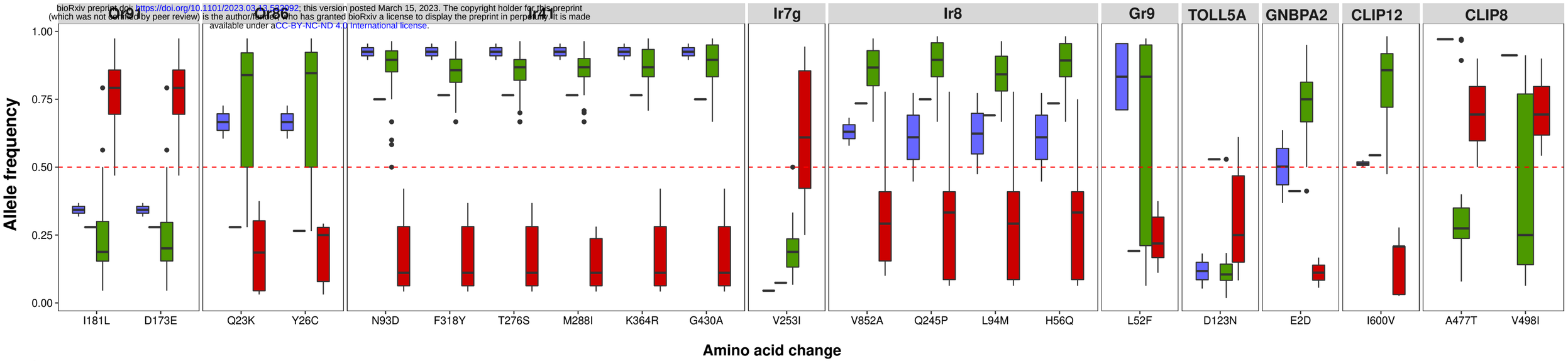

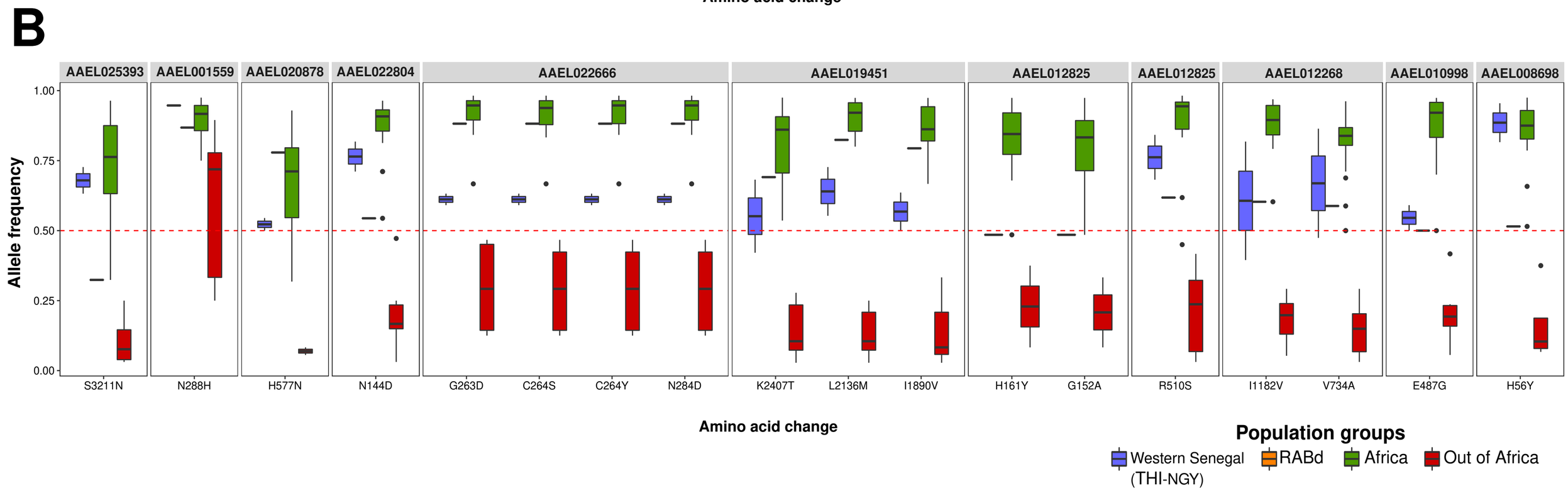

A

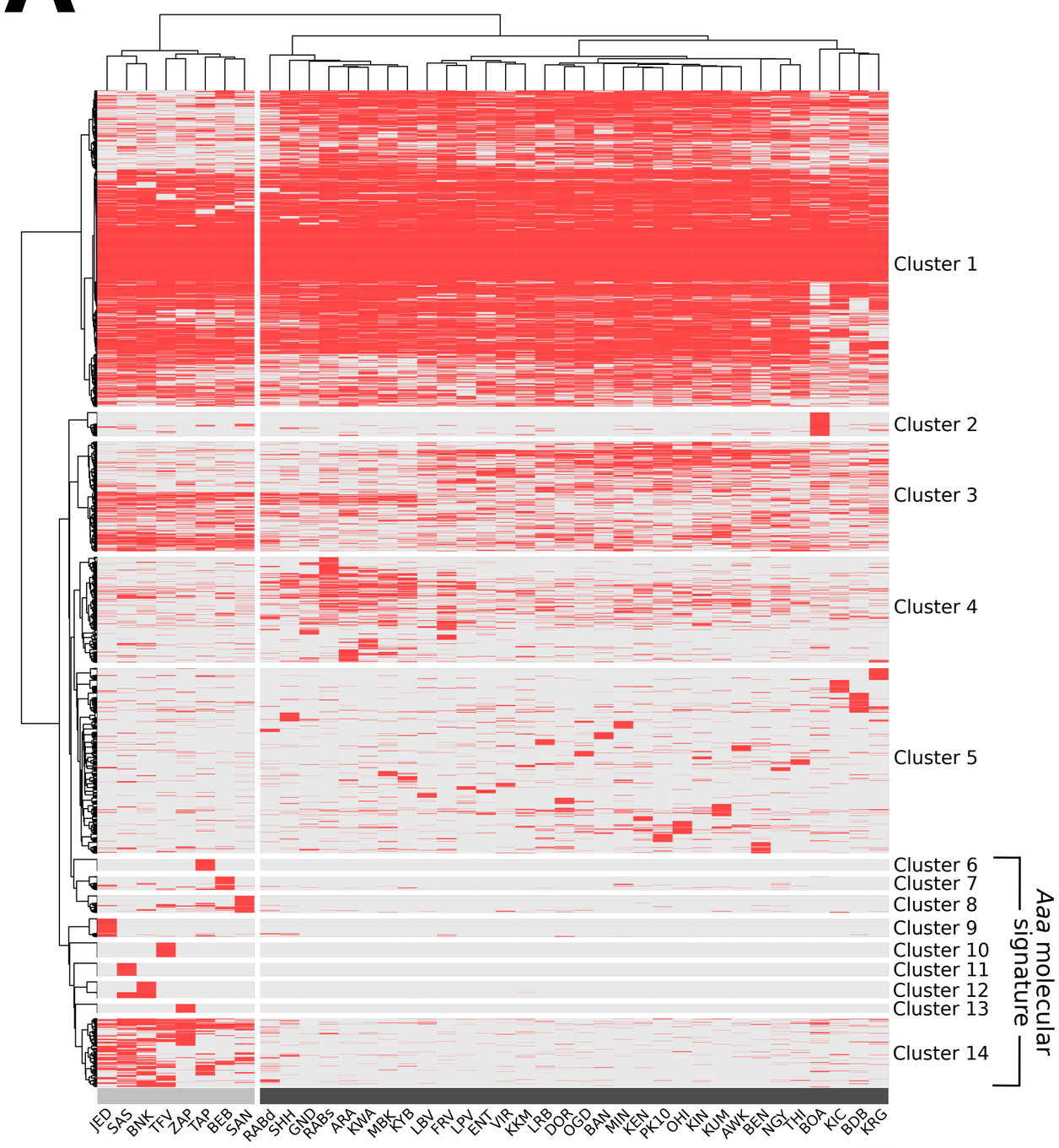

B

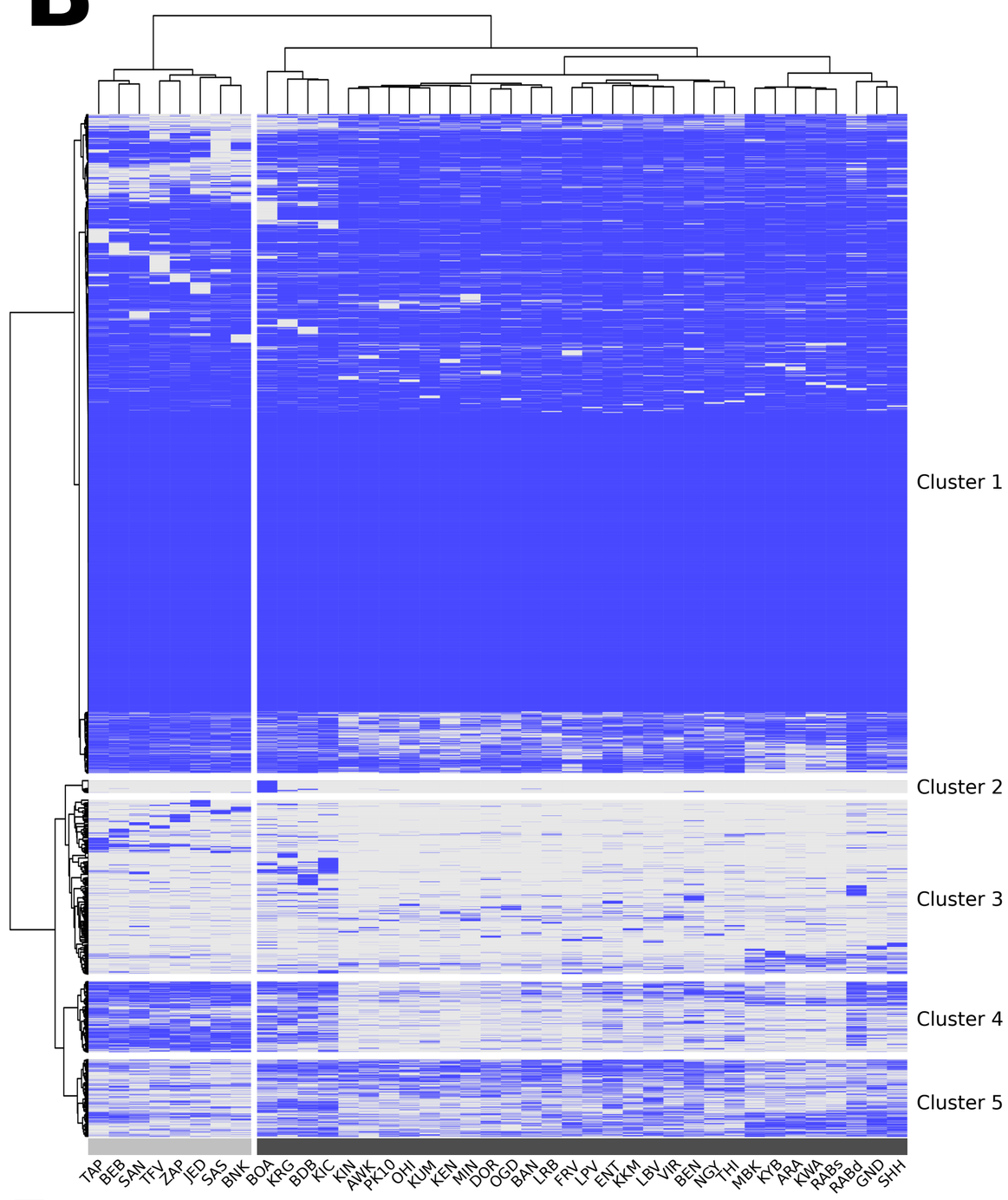

Out of Africa Africa

C

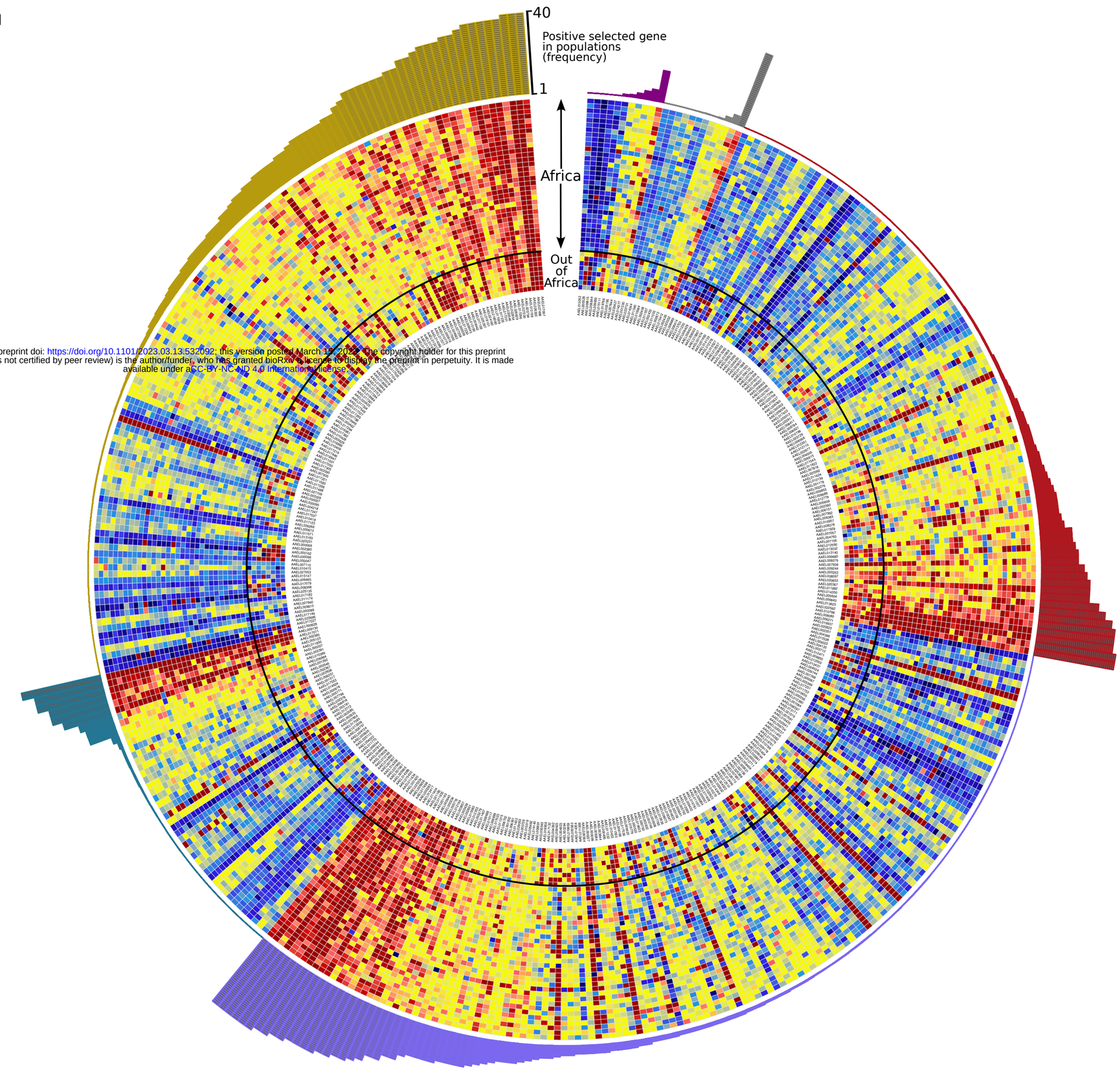

Gene Families

- Chemosensory receptors
- Detoxification
- Immunity
- Multigene family
- Proteases
- Metalloproteases

Ka/Ks ratio